Diana Xavier Cardoso Torres Gago

Bachelor of Science in Chemical and Biochemical Engineering

Evaluation of the adsorption capacity of a new cellulose-based polymer

Dissertation submitted in partial fulfillment
of the requirements for the degree of

Master of Science in
Chemical and Biochemical Engineering

Advisor: Isabel Maria Rôla Coelhoso,
Assistant Professor with Habilitation,
Universidade Nova de Lisboa

Co-advisor: Ricardo Alexandre Ventura das Chagas,
Post-Doctoral Researcher,
Universidade Nova de Lisboa

Examination Committee

Chair: Prof. Dr. Mário Fernando José Eusébio
Rapporteur: Prof. Dr. Isabel Maria de Figueiredo Ligeiro da Fonseca
Member: Prof. Dr. Isabel Maria Rôla Coelhoso

FACULDADE DE
CIÊNCIAS E TECNOLOGIA
UNIVERSIDADE NOVA DE LISBOA

September, 2019

Evaluation of the adsorption capacity of a new cellulose-based polymer

This document was created using the (pdf)LaTeX processor, based on the "novathesis" template[1], developed at the Dep. Informática of FCT-NOVA [2].
[1] https://github.com/joaomlourenco/novathesis [2] http://www.di.fct.unl.pt

Acknowledgements

Gostaria de expressar a minha gratidão a todos aqueles que de alguma forma contribuíram para a elaboração desta tese. Não há palavras suficientes que descrevam o meu agradecimento por toda a orientação, apoio e carinho que recebi.

À minha Orientadora, Professora Doutora Isabel Coelhoso, por me ter dado a oportunidade de participar neste projecto e, sobretudo, pela orientação ao longo deste semestre, transmissão de conhecimentos e simpatia. O seu empenho, disponibilidade e incentivo constante foram fundamentais na elaboração desta tese.

Ao meu Co-Orientador, Doutor Ricardo Chagas, pela incessante ajuda desde o primeiro dia. E pela bem-humorada paciência de todas as (muitas) vezes que surgi com questões e dúvidas novas.

À Professora Doutora Luísa Pinto Ferreira, minha Co-Orientadora em espírito, mesmo não sendo no papel. Obrigada por toda a partilha de conhecimentos e esclarecimento de dúvidas no decorrer deste trabalho, sempre com simpatia e boa disposição.

À D. Palminha e à D. Maria José, pela amabilidade e simpatia permanentes.

À Yana Hryno, aluna do Mestrado Integrado em Engenharia Química e Bioquímica, pela dedicada companhia nos primeiros meses de trabalho laboratorial. Foi uma ajuda preciosa.

Aos meus amigos dentro e fora da faculdade. À Sofia, pelo companheirismo e motivação na escrita da tese (e pelos vídeos de pandas e alpacas rechonchudos). À Rafaela, pela amizade duradoura e por estar sempre disponível para ouvir os meus desabafos e me animar.

Um agradecimento especial aos meus pais, pela paciência, afecto e apoio não só durante o meu percurso académico, mas ao longo de toda a minha vida. *J'avais du pain à la planche mais j'ai fait un tabac!*

Finalmente, ao Gonçalo, por me apoiar em todas as minhas decisões. Já são quase dez anos de momentos e etapas conquistadas juntos. Um obrigado também à tua família, pelo afecto com que sempre me presentearam.

"Science knows no country, because knowledge belongs to humanity, and is the torch which illuminates the world."

- Louis Pasteur

Abstract

A novel cellulose-based polymer, dicarboxymethyl cellulose (DCMC), was synthesized from cellulose and sodium 2-bromomalonate. Inductively coupled plasma atomic emission spectrometry (ICP-AES) and Fourier-transform infrared spectroscopy (FTIR) were employed to characterize the polymer. The size of the particles ranged between 10 and 100 μm.

Equilibrium and kinetic adsorption studies were performed to evaluate its suitability for methylene blue removal at different pH. Equilibrium adsorption data was analyzed using Langmuir and Freundlich isotherms. At pH = 3, adsorption isotherms followed the Langmuir model with a maximum adsorption capacity of 887.6 mg/g. At pH = 6.4, the adsorption isotherms produced an S-shape and were fitted with the Sips model, giving a maximum uptake of 1354.6 mg/g. Pseudo second-order kinetic model provided the best fit of the experimental data. The reusability of DCMC was evaluated. After the first cycle, adsorption decreased 30%. Adsorption coupled with membrane filtration allowed complete removal.

The adsorption of cytochrome C was evaluated. The adsorption process followed the Langmuir adsorption isotherm, giving a maximum uptake of 1279.6 mg/g. Pseudo second-order kinetic model adjusted well the experimental data. DCMC was successfully regenerated and reused without compromising performance. After three cycles, adsorption efficiency was above 90%.

Keywords: Adsorption isotherms, Adsorption kinetics, Dicarboxymethyl cellulose, Dye removal, Low-cost adsorbents, Protein purification.

Resumo

Um polímero derivado de celulose, dicarboximetil celulose foi preparado com celulose e ácido bromomalónico e a sua capacidade de adsorção de pigmentos (azul de metileno) e proteínas (citocromo *C*) foi estudada. O polímero foi caracterizado por técnicas de espectrometria de emissão atómica (ICP-AES) e de infravermelho (FTIR).

Foram realizadas experiências de equilíbrio e cinética a diferentes valores de pH, de modo a avaliar a remoção de azul de metileno. A pH = 3, obtém-se uma capacidade máxima de adsorção de 887.6 mg/g, ajustando a isotérmica de Langmuir. A pH = 6.4, as isotérmicas produzem uma curva em S e foram ajustadas usando o modelo de Sips, obtendo-se um valor máximo de 1354.6 mg/g de adsorção. Os resultados foram descritos pelo modelo cinético de pseudo segunda-ordem. A reutilização do polímero foi estudada. Após o primeiro ciclo de adsorção-dessorção, a adsorção foi reduzida em 30%. Adsorção acoplada a filtração com membranas permitiu uma completa remoção do pigmento.

A adsorção de citocromo *C* foi também avaliada observando-se uma capacidade máxima de adsorção de 1279.6 mg/g. Os resultados foram descritos pelo modelo cinético de pseudo segunda-ordem. O polímero foi regenerado e reutilizado sem alterações no seu desempenho. Após três ciclos, a eficiência de remoção foi superior a 90%.

Palavras-chave: Adsorventes de baixo-custo, Cinética de adsorção, Dicarboximetil celulose, Isotérmicas de adsorção, Remoção de pigmentos, Separação de proteínas.

Contents

List of Figures

List of Tables

Chapter 1

Introduction

1.1 Background and motivation

The adsorption process has been known for a long time. Processes which are now associated with adsorption have been depicted in literature over the past two millenia (Rouquerol et al., 2013).

Adsorption is an important separation process, widely used in industrial applications (Tien, 2018). This surface phenomena occurs when a solid substance (adsorbent) is exposed to a gas or liquid (adsorbate) (Rouquerol et al., 2013). Desorption is the reverse process, where accumulated molecules are released from the surface of the adsorbent (Dąbrowski, 2001; Everett, 1972). Adsorption differs from absorption which in turn refers to a bulk phenomenon where molecular species penetrate the absorbing solid rather than accumulating at the surface (Gregg and Sing, 1991; Tien, 2018).

The adsorption process is characterized based on the interactions between solid adsorbent and adsorbed molecules and the strength of the bonds between them (Bansal and Goyal, 2005; Dąbrowski, 2001). Adsorption types are defined as physisorption or chemisorption (Dąbrowski, 2001; Rouquerol et al., 2013).

In physisorption, van der Waals and/or electrostatic forces are responsible for the bond between adsorbent and adsorbate (Choi et al., 2001). Since there are no chemical bonds involved, a physisorbed molecule usually returns to its previous form when desorbed (Choi et al., 2001). Compared to chemical adsorption, physisorption has low heat of adsorption (1-2 versus 10-100 kcal/mol, respectively) (Bhushan, 2013; Rouquerol et al., 2013). The physisorption process is always exothermic (Rouquerol et al., 2013).

Chemisorption is a process with chemical specificity that results from the electron exchange between adsorbent and adsorbate (Bhushan, 2013; Dąbrowski, 2001; Everett,

1972; Gregg and Sing, 1991). Chemisorbed molecules suffer alterations to their electronic structure making their recovery impossible after desorption (Choi et al., 2001). Chemical and physical adsorption can occur simultaneously (Dąbrowski, 2001). Since, chemisorption is necessarily a monolayer adsorption process, after the surface is fully covered, chemisorption ceases and subsequent layer formation may occur by physisorption (Bhushan, 2013; Choi et al., 2001).

The type of accumulation of adsorbed molecules onto the adsorbent is defined as monolayer or multilayer (Everett, 1972). In monolayer adsorption (see Figure 1.1a) all adsorbed molecules are in contact with the surface layer (Everett, 1972). In multilayer adsorption (see Figure 1.1b), as the name suggests, adsorbed molecules are distributed in several layers (Everett, 1972).

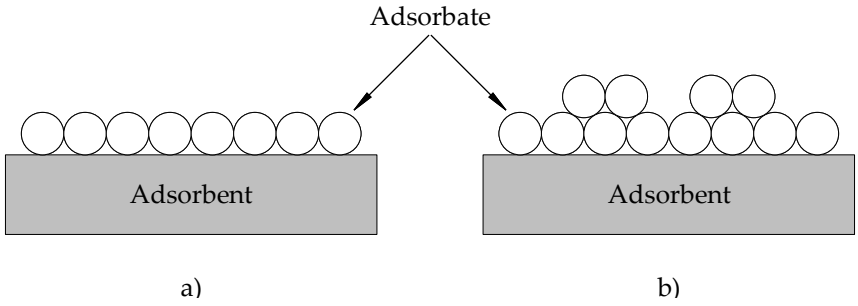

Figure 1.1: Schematic of the a) monolayer and b) multilayer adsorption process

Similarly to adsorption, ion exchange is a separation process where there is mass transfer from fluid to solid phase (Cobzaru and Inglezakis, 2015; Tien, 2018). However, in ion exchange, as the name implies, there is an actual exchange process (Cobzaru and Inglezakis, 2015). This process is characterized by electrostatic interactions between the functional groups of the adsorbent and charged ions in the fluid (Cobzaru and Inglezakis, 2015; Ståhlberg, 1994; Tien, 2018). Ion exchange materials are water-insoluble polyelectrolyte solids with functional active groups able to perform ionic exchange (Cobzaru and Inglezakis, 2015).

New types of adsorbents have been developed over the past few decades (Rouquerol et al., 2013; Tien, 2018). Adsorbent characteristics such as shape, porosity and surface area have direct influence on adsorption capacities (Tsai et al., 2008). According to IUPAC, adsorbents are defined based on pore internal width as micropores (> 2 mm), mesopores (between 2 and 50 mm) and macropores (< 50 mm) (Dąbrowski, 2001; Everett, 1972; Rouquerol et al., 2013). Some of the most widely used adsorbents are activated carbons, aluminas and silica gels(Rouquerol et al., 2013; Tien, 2018). However, growing environmental awareness has boosted the search for environmentally-friendly alternatives to conventional adsorbents (Kyzas and Kostoglou, 2014).

With an estimated annual production of 1.5×10^{12} tons, cellulose is considered an almost inexhaustible material source (Klemm et al., 2005). Cellulosic materials have been used for the last 150 years (Klemm et al., 2005). The need for renewable resources and

environmentally-friendly materials has fueled the research on cellulose-based products (Klemm et al., 2005; Missoum et al., 2013; Xin et al., 2017). Chemical modification of hydroxyl groups creates cellulose derivatives with new properties and applications (Klemm et al., 2005). Cellulose derivatives, such as carboxymethyl cellulose and hydroxyethyl cellulose, are already being used at an industrial scale (Chagas et al., 2019; Klemm et al., 2005; Nasatto et al., 2015; Roy et al., 2009).

The development of a novel cellulose-based polymer is of great importance for the scientific community (Klemm et al., 2005). The synthesis of dicarboxymethyl cellulose has been described by Diamantoglou et al., 1977 and recently by Chagas et al., 2019; Ferreira et al., 2019. Dicarboxymethyl cellulose (DCMC) results from the introduction of a substituent with two carboxylic acid groups (Chagas et al., 2019). The heterogeneous etherification of cellulose with a low pKa acid results in a polymer that can perform ion-exchange at low pH (Chagas et al., 2019; Diamantoglou et al., 1977; Ferreira et al., 2019). Therefore, DCMC has the potential to be a relevant ion-exchanger with a wide pH working window (Chagas et al., 2019).

The use of cellulose derivatives in industrial sectors such as wastewater treatment and pharmaceutics is widely reported (Heinze et al., 2018; Klemm et al., 2005; Sun et al., 2019). The presence of dyes and pigments in wastewaters is a major environmental problem (Aksu, 2005). Recovery and immobilization of proteins can also be achieved by electrostatic interactions between adsorbent and adsorbate (Feng et al., 2009; Miyahara et al., 2007). Adsorption and ion exchange are common techniques used in both industries (Bellezza et al., 2009; Cobzaru and Inglezakis, 2015; Harrison et al., 2015; Miyahara et al., 2007; Novais et al., 2018b; Rafatullah et al., 2010). Adsorption capacity depends on the availability of exchangeable cations of the adsorbent (Kahr and Madsen, 1995).

The protein removal capacity of DCMC has already been tested in white wine proteins by Ferreira et al., 2019. Commercial value of white wines is reduced by the appearance of sedimentation and turbidity (Colangelo et al., 2018; Vela et al., 2017). The presence of positively-charged wine proteins contributes to haze formation (Ferreira et al., 2019; Van Sluyter et al., 2015; Vela et al., 2017). The ability to perform cation exchange at low pH is useful in white wine clarification and stabilization (Ferreira et al., 2019). Subsequent filtration without lees formations presents significant advantages over currently used conventional fining agents (Ferreira et al., 2019).

LAQV-REQUIMTE is responsible for the synthesis of dicarboxymethyl cellulose. An interest in studying this polymer as an adsorbent motivated this Master's thesis. Characterization of DCMC as a novel cellulose-based polymer will be addressed. The potential of DCMC for wastewater treatment and protein removal is investigated through adsorption experiments using a cationic dye and protein models.

1.2 Thesis Outline

This thesis is divided into five chapters, following the work performed throughout this project. Each chapter is self-contained and describes the materials and methods used, the discussion of results and main conclusions. The methodology used in each individual chapter is detailed and, when applicable, is related to that used in previous chapters. The work performed during this Master's thesis and presented in Chapter 3 has resulted in a scientific article, which will be submitted for publication in the special issue *Membrane Processes and Materials for a Sustainable Bioeconomy* of the Journal Membranes (MDPI).

- **Chapter 1** introduces the key concepts of the work developed and explains the motivation behind this dissertation.
- **Chapter 2** presents the polymer used in this work, covers its synthesis and characterization, with techniques such as Inductively Coupled Plasma Atomic Emission Spectrometry and Fourier Transform infrared spectroscopy.
- **Chapter 3** studies the adsorption of a common cationic dye, methylene blue.
- **Chapter 4** reports the adsorption experiments of cytochrome *C*.
- **Chapter 5** presents the final remarks and main conclusions of this thesis, discussing them in an integrated way. Suggestions for future research are also presented.

Chapter 2

Synthesis and characterization of the cellulose-based polymer

2.1 Summary

A novel cellulose-based polymer has been synthesized from cellulose and sodium 2-bromomalonate (BMA). Number of carboxylate groups per gram of polymer (CG) was controlled by altering reaction conditions, namely the molar ratio between BMA and cellulose. Three polymers were prepared differing in the amount of BMA added. Inductively coupled plasma atomic emission spectrometry (ICP-AES) and Fourier-transform infrared spectroscopy (FTIR) were employed to characterize the structure of the cellulose-based adsorbent. CG was calculated with sodium content determined by ICP-AES. Adjusting BMA molar equivalents increased functionalization obtaining a CG between 0.15 and 0.30 ($mmol_{Na}/g_{pol}$). Absorption spectra revealed an intensity increase of the peaks associated with carbonyl stretching of ester groups and carboxylate groups with higher CG. Optical microscopy was used to observe the morphology of the polymer. Quantitative analysis of the images was performed using ImageJ. The synthesized polymer is an irregularly-shaped flowing fine white powder. The length of dicarboxymethyl cellulose particles ranged between 10 and 100 μm. Surface areas of 208, 6284 and 7415 μm^2 were obtained for the three polymers.

2.2 Introduction

Cellulose is the most abundant regenerated material on Earth (Kirk-Othmer, 2005). It is estimated that 1.5×10^{12} tons of cellulose are produced every year (Klemm et al., 2005). On account of being biodegradable, renewable and readily available, this polysaccharide is already commonly used in the chemical industry (Onwukamike et al., 2019; Varshney

and Naithani, 2011). Moreover, the use of cellulose in the chemical industry follows the Green Chemistry principle promoting the use of renewable feedstock as an alternative to non-renewable raw materials (Anastas and Eghbali, 2010). Cellulose and its derivatives are used in broad applications, such as optical films, fiber, coatings, plastics, pharmaceutical and biomedical materials (Vilela et al., 2010; Xiao et al., 2014). Different cellulose derivatization techniques are used to introduce the desired physical and chemical properties (Chagas et al., 2019; Xiao et al., 2014).

Cellulose is a homopolymer generated from repeating β-D-gluco-pyranose molecules covalently linked through acetal functions between the equatorial OH group of C4 and the C1 carbon atom (β-1,4-glycosidic bonds) (Klemm et al., 2005; Onwukamike et al., 2019; Roy et al., 2009). The chemical structure and spatial arrangement of cellulose (see Figure 2.1) influence its chemical and physical properties (Kirk-Othmer, 2005; Roy et al., 2009). Homogeneous and heterogeneous derivatization methods are used to change or introduce new characteristics to the polymer (Chagas et al., 2019; Xiao et al., 2014). Derivatization methods include chemical modification to the hydroxyl groups (three per anhydroglucose unit), namely substitution by specific chemical agents (Onwukamike et al., 2019; Wuestenberg, 2014). The average number of OH groups substituted are defined as degree of substitution (DS) and may therefore range from zero to three (Roy et al., 2009; Wuestenberg, 2014). Degree of polymerization (DP) is the chain length of cellulose (Klemm et al., 2005; Varshney and Naithani, 2011). This property can be regulated by the source and treatment of the raw material (Klemm et al., 2005).

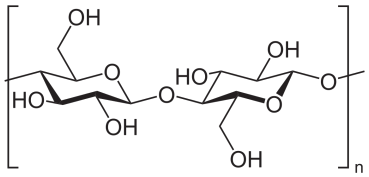

Figure 2.1: Chemical structure of cellulose (n is the degree of polymerization)

Functionalization can be achieved through multiple processes, such as phosphorylation, esterification and etherification (Onwukamike et al., 2019; Varshney et al., 2006). The etherification process is used for modifications of the cellulose structure (Roy et al., 2009). Cellulose etherification consists of reactions of cellulose with alkylating agents, namely dicarboxylic acids, in the presence of a base and inert diluent (Diamantoglou et al., 1977; Kirk-Othmer, 2005; Roy et al., 2009). Among the commonly studied cellulose ethers are carboxymethyl cellulose (CMC), methyl cellulose and hydroxyethyl celluloses (Kirk-Othmer, 2005; Roy et al., 2009). However, most of these derivatives have low pH working windows (Chagas et al., 2019). The synthesis of a cellulose-based polymer with lower pKa has the potential to be a relevant ion-exchanger with a larger pH range (Chagas et al., 2019).

In this work, we present a cellulose-based polymer prepared by heterogeneous etherification with bromomalonic acid (Diamantoglou et al., 1977; Ferreira et al., 2019; Kötz

et al., 1991). To complete the reaction, a common base (NaOH) used in the manufacture of cellulose ethers is added (Diamantoglou et al., 1977; Ferreira et al., 2019; Kirk-Othmer, 2005). The polymer is cross-linked by heat treatment to achieve insolubilization in aqueous solutions (Ferreira et al., 2019). The conditions imposed on the synthesis of the polymer determine degree of polymerization, number of carboxylate groups per gram of polymer and molecular weight. The polymer is characterized by optical microscopy, Inductively coupled plasma atomic emission spectrometry (ICP-AES) and Fourier transform infrared spectroscopy (FTIR). ICP-AES is a common method for qualitative and quantitative element analysis (Moore, 2012). This technique is used for single-element analysis due to its simplicity and accuracy. Elements in a sample are excited, using plasma, emitting radiation of a characteristic wavelength, which is matched with emission lines of known elements (Thompson, 2012). FTIR is widely used for analysis of absorption spectra (Rehman and Bonfield, 1997; Smith, 2011). There are established correlations between peak positions and molecular structures (Smith, 2011). This technique is useful for spectral comparison, namely identifying the different peak positions, heights and widths (Smith, 2011). Attenuated total reflectance (ATR) provides an easy method of obtaining polymer absorption spectra (Devasahayam et al., 2016; Smith, 2011). ATR spectroscopy relies on the optical contact of the polymer with the reflection element, thus avoiding techniques which could alter the morphology of the sample (Devasahayam et al., 2016; Smith, 2011).

2.3 Materials and Methods

2.3.1 Materials

Air-dry cellulose (MN 400 Avicel) was obtained from Macherey-Nagel. Sodium bromomalonate was previously synthesized by LAQV - REQUIMTE with bromine and malonic acid. Other chemicals and solvents were of laboratory grades and used without further purification.

2.3.2 Methods

2.3.2.1 Synthesis of dicarboxymethyl cellulose

Cross-linked dicarboxymethyl cellulose (DCMC) was synthesized specifically for this work in LAQV - REQUIMTE, Departamento de Química, Faculdade de Ciências e Tecnologia, Universidade Nova de Lisboa.

Three different polymers were prepared, differing in the amount of sodium 2-bromomalonate (BMA) added. To produce polymers with varying number of carboxylate groups, BMA was added in 1, 2 and 3 equivalent moles of anhydroglucose units (AGU). The reaction was controlled to avoid changes in degree of polymerization (DP), which depends on cellulose chain length (number of AGU) (Klemm et al., 2005; Varshney and

Naithani, 2011). DP affects mechanical and physiological properties, such as viscosity of solutions (Furia, 1973; Varshney and Naithani, 2011). DCMC was synthesized following the procedure described by Chagas et al., 2019; Ferreira et al., 2019. Figure 2.2 is a schematic representation of the reaction between cellulose and bromomalonic acid.

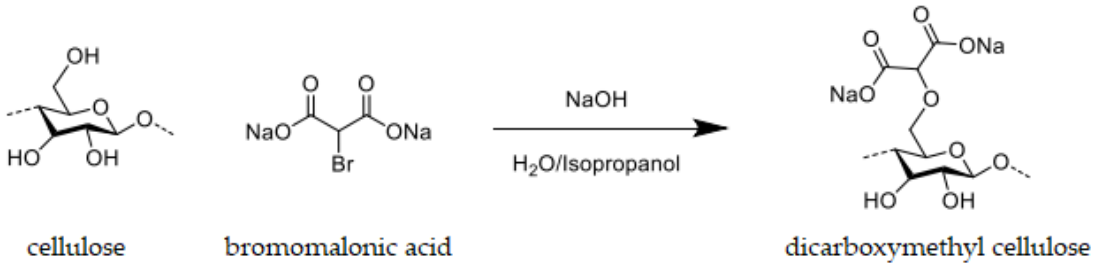

Figure 2.2: Schematic representation of the synthesis of dicarboxymethyl cellulose

5 g of air-dry cellulose and 175 mL isopropanol were stirred vigorously and 5.5 mL of a 40% (w/v) aqueous NaOH solution was slowly added to the mixture for 10 min at room temperature. The mixture was magnetically stirred for 1 h and the appropriate quantity of sodium 2-bromomalonate in 18 mL of water was added. After complete homogenization, the mixture was placed on a water bath at 60 °C for 3 to 5 h with vigorous stirring. After this time, the reaction mixture was filtrated, and the solid suspended in 70% (v/v) methanol and neutralized with acetic acid. Aqueous and pure methanol were used for further purification of the product. Finally, the product dried under vacuum at room temperature. The latter was protonated dispersing the powdered product in 20% sulfuric acid solution for 1 h. The product was decanted and the precipitate washed with distilled water until neutral pH. After drying, the protonated polymer was heated at 100 °C for 1 h promoting its cross-linking by esterification (formation of ester bonds between the carboxylic acid of the malonate group and the hydroxyl group of adjacent cellulose chains). The resulting cross-linked polymer was washed with 1 M NaCl until neutral pH followed by washing with distilled water to remove remaining NaCl. The sodium salt of the cross-linked polymer was isolated by filtration and dried under vacuum yielding a white powder. Table 2.1 shows the appropriate quantities of each reagent for the synthesis of dicarboxymethyl cellulose in these conditions (Chagas et al., 2019).

Table 2.1: Conditions for the synthesis of dicarboxymethyl cellulose

Samples	BMA eq. [a]	AGU (g) [b]	IP (mL) [c]	NaOH (g)	BMA (g) [d]
DCMC 1	1	5.0	175	3.68	6.95
DCMC 2	2	5.0	175	3.68	13.91
DCMC 3	3	5.0	175	3.68	20.86

[a] Sodium bromomaloate equivalents to anhydroglucose unit
[b] Anhydroglucose units
[c] Isopropanol
[d] Bromomalonic acid

2.3.2.2 Morphology and size distribution of the synthesized DCMC

Morphology and size distribution of dicarboxymethyl cellulose were analyzed by optical microscopy with a Nikon Eclipse ci. The images were processed with ImageJ software. No treatment was applied to the polymer in order to have uniform particle size.

2.3.2.3 Sodium content determination by ICP-AES

The analysis was carried out for all polymers to determine the influence of stoichiometry on the chemical structure. The samples were prepared by adding 500 μl nitric acid to a known mass of polymer (approximately 1.0 mg). Then, they were incubated at 70 °C for 1 h. Differences in sodium content were assessed by ICP-AES. Quantification of carboxylate functional groups is based on the ionic exchange between sodium ions and carboxyl groups.

2.3.2.4 Characterization of chemical structure and functional groups

The analysis was carried out for all polymers to determine the influence of stoichiometry on the chemical structure. FTIR was recorded on a Perkin-Elmer FT-IR Spectrometer Spectrum Two, equipped with an attenuated total reflection (ATR) cell, in the range of 4000 to 400 cm^{-1}.

2.4 Results and Discussion

2.4.1 Morphology and size distribution of the synthesized DCMC

Dicarboxymethyl cellulose was synthesized with the previously described method. The final product of the three polymers can be observed in Figure 2.3. Dicarboxymethyl cellulose is a flowing fine white powder.

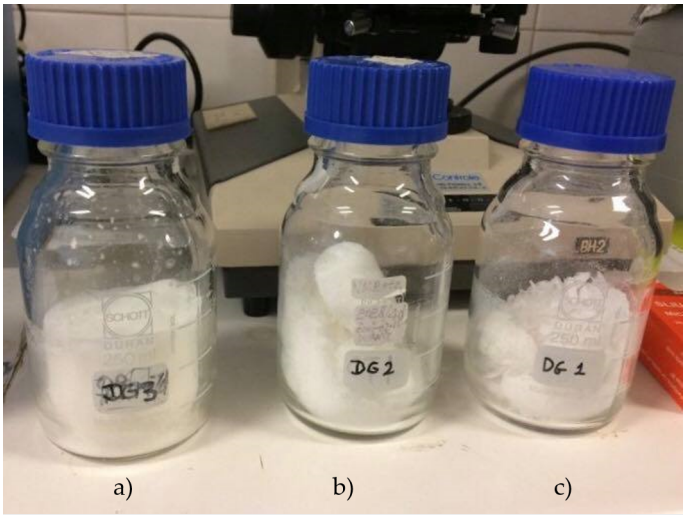

Figure 2.3: Picture of a) DCMC 3, b) DCMC 2 and c) DCMC 1.

Pictures of the polymer obtained by optical microscopy are displayed in Figure 2.4. From Figure 2.4, the polymer has an irregular shape and seems to be aggregated. No further analysis was performed on these particles.

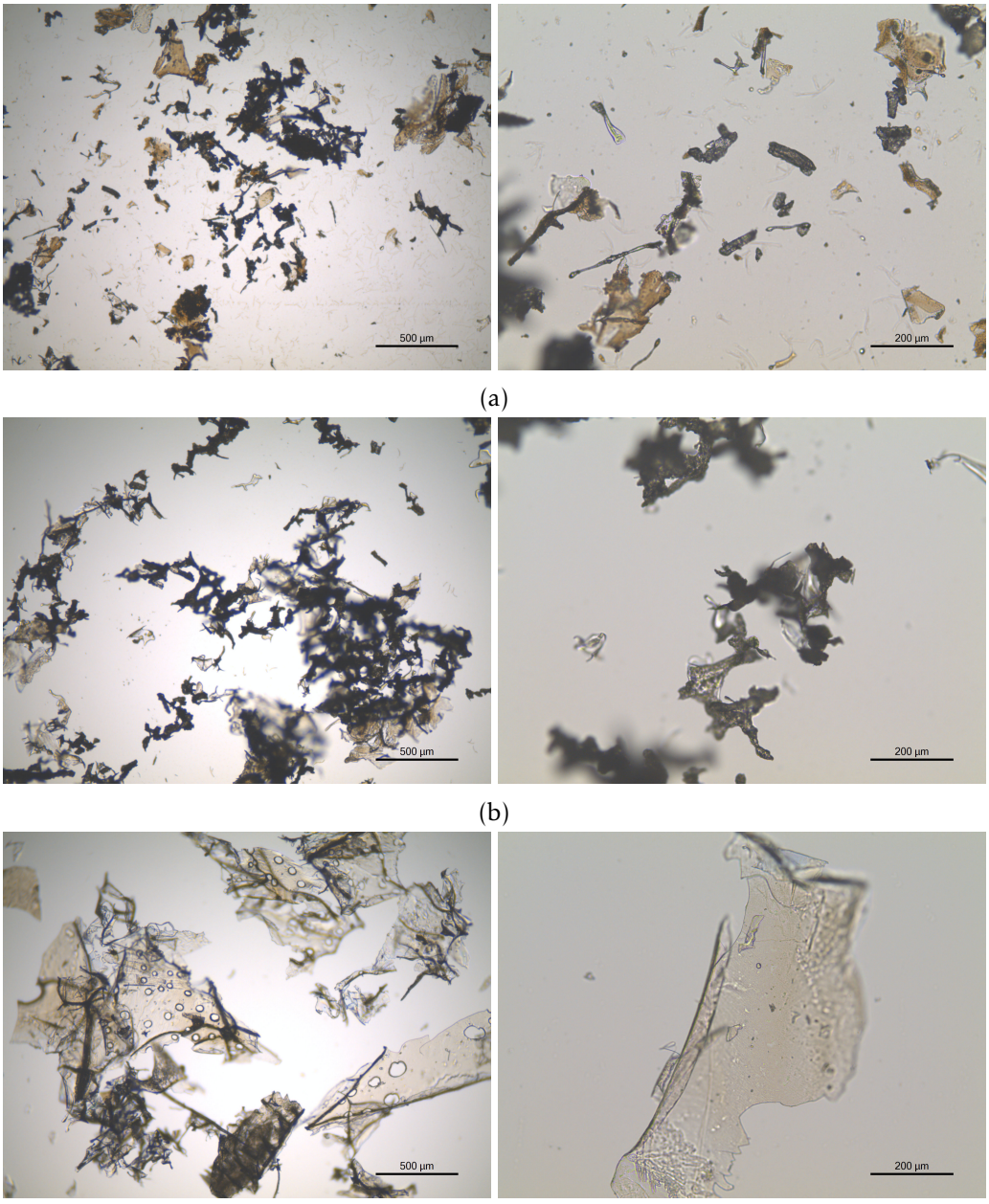

Figure 2.4: Optical microscopy images of a) DCMC 1, b) DCMC 2 and c) DCMC 3.

To disrupt aggregation, the polymer was mixed with deionized water. The images obtained with the polymer in aqueous solution are shown in Figure 2.5. Based on Figure 2.5, the polymer doesn't have a defined shape. To the naked eye, the different polymers all look similar. However, after analyzing the images obtained by optical microscopy, the particle size distribution varies with the number of carboxylate units per gram of DCMC.

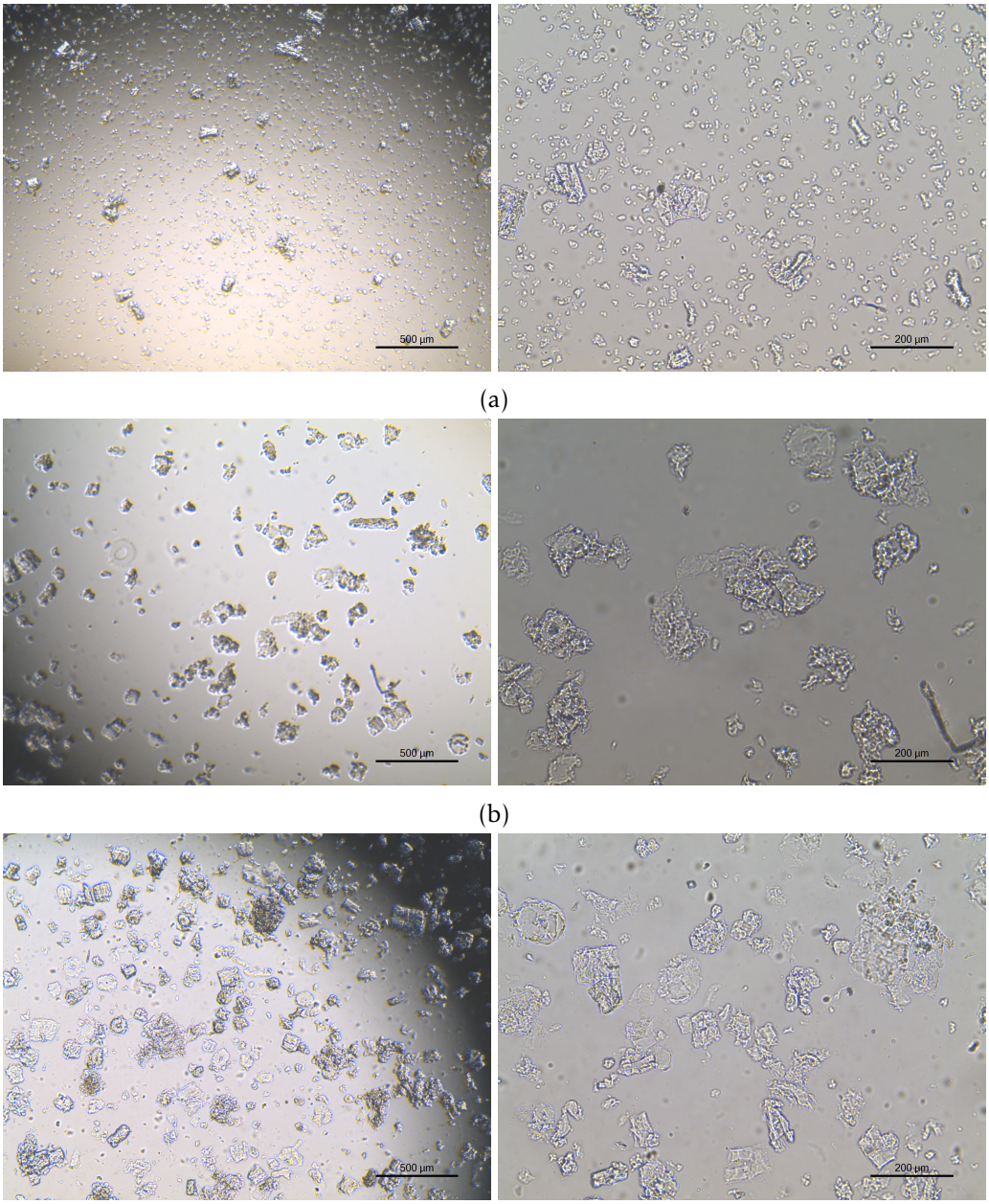

Figure 2.5: Optical microscopy images of dicarboxymethyl cellulose in aqueous solution: a) DCMC 1, b) DCMC 2 and c) DCMC 3.

The calculated dimensions for the polymers are presented on Table 2.2. Using ImageJ, length was measured by extending a line for the length of the polymer. Surface area was calculated by the software when delimiting the particles. DCMC 1 is considerably smaller than DCMC 2 and DCMC 3. Contrarily, there are no significant differences in the dimensions of DCMC 2 and DCMC 3.

Table 2.2: Dimensions of dicarboxymethyl cellulose

Samples	Length (μm)	Surface area (μm^2)	Volume (μm^3)	SA/V (μm^{-1})[a]
DCMC 1	14.0±4.5	207.7±141.2	1 451.3±46.3	0.143
DCMC 2	77.5±26.8	6 284.1±3 948.6	244 057.4±10 025.7	0.026
DCMC 3	78.2±21.5	7 415.0±2 490.5	250 468.0±5 205.9	0.030

[a] Surface area to volume ratio

2.4.2 Sodium content determination by ICP-AES

The sodium content in dicarboxymethyl cellulose samples was determined by ICP-AES. Percentage of sodium in each sample is the quotient of sodium and polymer mass. The number of carboxylate groups per gram of polymer (CG) was calculated by Equation (2.1). Each sodium atom corresponds to a carboxylate unit able to perform the desired ionic exchange. As expected, with increasing sodium 2-bromomalonate in the polymer synthesis there is an increase in this number.

$$CG = \frac{\frac{\%Na}{100} \times 1000}{23} \tag{2.1}$$

where the term "23"represents the molecular mass of sodium (g/mol).

Table 2.3: Results of the synthesis of dicarboxymethyl cellulose

Samples	C_{Na} (mg/l)	m_{pol} (mg)	m_{Na} (mg)	% Na	CG ($mmol_{Na}/g_{pol}$)[a]
DCMC 1	9.69	1.3	0.0048	0.37	0.1620
DCMC 2	10.45	1.2	0.0052	0.44	0.1894
DCMC 3	12.43	1.0	0.0062	0.62	0.2703

[a] Carboxylate groups per gram of polymer

2.4.3 Characterization of chemical structure and functional groups

FTIR is used to characterize the chemical structure and functional groups. Figure 2.6 shows the absorption spectra of the different dicarboxymethyl cellulose polymers.

A broad adsorption peak at 3300 cm^{-1} is in the range of -OH stretching vibration (Lin et al., 2017; Saber-Samandari et al., 2016). A decrease of intensity with a higher number of carboxylate groups (CG) could be justified by a breakage of hydrogen bonds. However, DCMC 3 has a higher intensity than DCMC 2. The difference in intensity could

be explained by ATR spectra sensibility to applied pressure. A change in pressure or force while measuring a solid sample may change its physical state, affecting the intensity of the absorption peak (Friedrich and Weidler, 2010; *Perkin-Elmer Manual*). The peak at 2890 cm^{-1} is attributed to the C-H stretching vibration (Lin et al., 2017; Saber-Samandari et al., 2016). The intensity of a band at 1720 cm^{-1}, which is related to the carbonyl stretching of the ester groups, increased with number of carboxylate groups per gram of polymer since the ester groups are formed during the cross-linking procedure. With a higher number of carboxylic acid groups an increase of the ester groups can be expected. The bands at 1615 cm^{-1}, 1420 cm^{-1} (COO^- symmetric) and 1330 cm^{-1} (C-O stretching) are also characteristic of the C=O bond stretching absorption (Lin et al., 2017). This functional group is present in carboxylate groups (COO^-). The asymmetric band increases in the presence of carboxylate groups (COO^-), which explains the increase in intensity with higher number of carboxylate groups per gram of polymer. Strong broad peaks at approximately 1100 and 1020 cm^{-1} indicate the presence of C-O-C bonds, characteristic of the cellulose backbone (Yan et al., 2011).

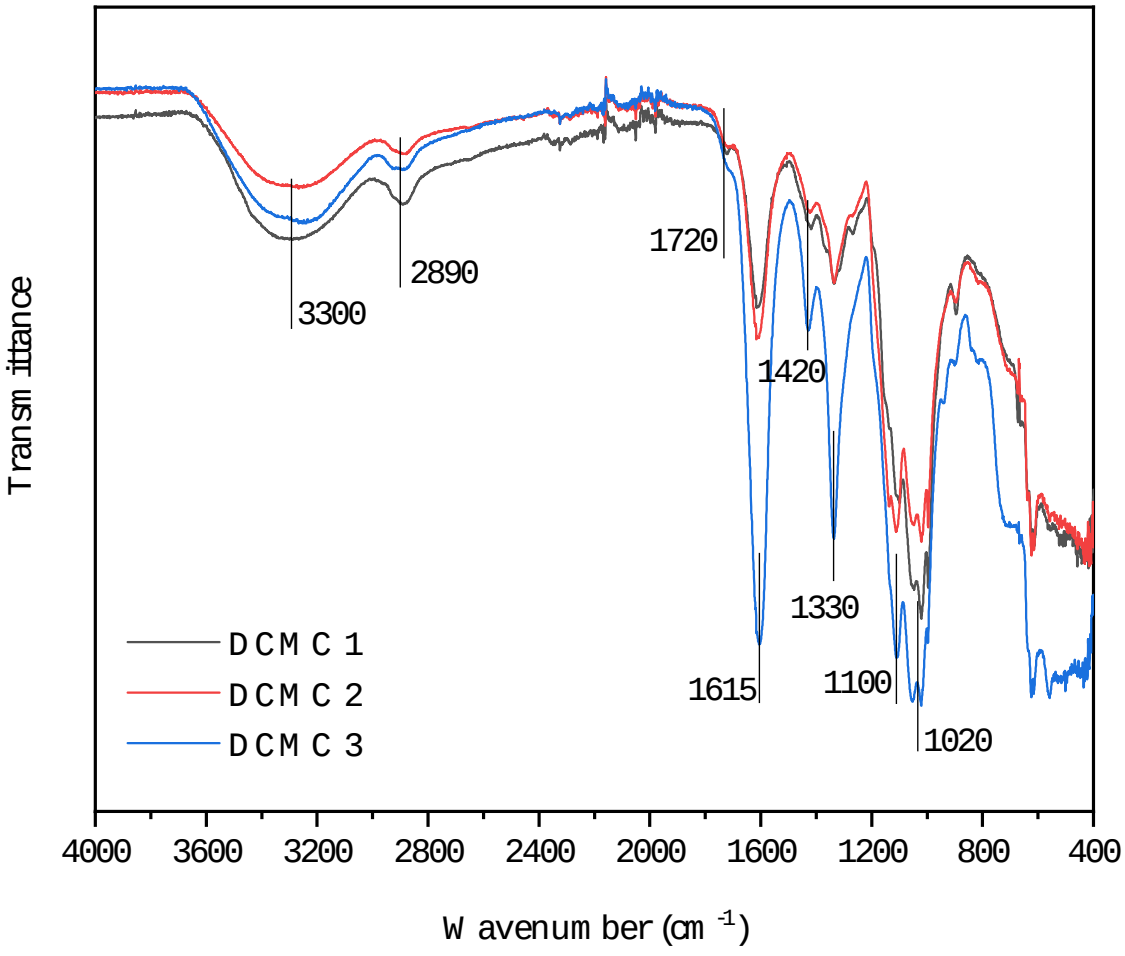

Figure 2.6: FTIR-ATR spectra of dicarboxymethyl cellulose

2.5 Conclusions

The synthesis of a new cellulose-based polymer was successful. Dicarboxymethyl cellulose produced will be characterized as an adsorbent to positively charged species with industrial interest.

Adjusting the number of sodium 2-bromomalonate (BMA) equivalents in the synthesis increased functionalization. FTIR and ICP provided information on the effect of BMA equivalents in the chemical structure of the polymer. As expected, increasing BMA increases the number of carboxylate groups per gram of polymer (CG). A correlation between CG and surface area to volume ratio was not established. Surface area to volume ratio was 0.143, 0.026 and 0.030 for the polymer synthesized with one, two and three BMA equivalents. The particle size length was determined to be 14.0, 77.5 and 78.2 μm for DCMC 1, DCMC 2 and DCMC 3, respectively.

The polymer should be further characterized by techniques such as scanning electron microscopy (SEM) and solid state nuclear magnetic resonance (NMR) since the polymer is insoluble in any tested solvent. Standardization of polymer size via mechanical processes should be considered as it may influence adsorption capacity based on available surface area.

Chapter 3

Adsorption of Methylene Blue

3.1 Summary

A novel cellulose-based polymer, dicarboxymethyl cellulose (DCMC), was used for methylene blue (MB) removal. A series of equilibrium and kinetic adsorption studies were performed to assess its suitability for dye removal. Effect of pH on adsorption capacity was studied. Experimental results from the studied range indicated that maximum adsorption capacity increases linearly with the number of carboxylate functional groups per gram of polymer. The equilibrium adsorption data were analyzed using two widely applied isotherms: Langmuir and Freundlich. At pH = 3, adsorption isotherms followed the Langmuir model with a maximum adsorption capacity of 887.6 mg/g, implying a homogeneous monolayer adsorption. Pseudo first-order and pseudo second-order models were used to fit the experimental data. Pseudo-second-order kinetic model provided the best correlation with the experimental data for the adsorption of MB onto DCMC, indicating a chemisorption process. The adsorption process is almost instantaneous, with more than 50% removal efficiency after 30 seconds with a low dosage of polymer. At pH = 6.4, the adsorption isotherms produced an S-shape and were fitted with the Sips model, with high correlation coefficients. The maximum MB uptake was 1354.6 mg/g at 25 °C and pH = 6.4. The reusability of DCMC was evaluated. Cycles of adsorption-desorption showed significant changes in both adsorption and desorption efficiency. A loss in adsorption performance may be explained by heat-induced cross-linking, reducing available binding sites. The use of a weak eluent agent did not effectively desorb methylene blue from dicarboxymethyl cellulose. After the first cycle, adsorption decreased from 84.7 to 33.8% in an experiment where the polymer was dried, and 84.6 to 56.0% when the polymer was washed between cycles without being heated.

3.2 Introduction

Dyes and pigments are used in several chemical industries, such as pharmaceutical and textile. These industrial processes require large volumes of water and are responsible for the annual release of up to 150 000 tons of dyes into wastewaters (Novais et al., 2018b). The presence of dyes in wastewaters is easily recognized by human eye, due to a change of colour, and may have dire effects on aquatic life and compromising photosynthetic activity of certain aquatic species (Aksu, 2005). Moreover, these pollutants are generally resistant to biodegradation because of their complex aromatic structures (Aksu, 2005). Methylene blue (see Figure 3.1) is a common representative of cationic dyes (Liu et al., 2018). It is typically used in the textile industry, for dying cotton and silk (Rafatullah et al., 2010). Numerous reports are available in the literature concerning the removal of this specific dye. Environmental awareness and regulatory measures contribute to a growing interest on cheaper and more effective techniques for the treatment of wastewaters containing dyes (Liu et al., 2018; Novais et al., 2018b; Rafatullah et al., 2010).

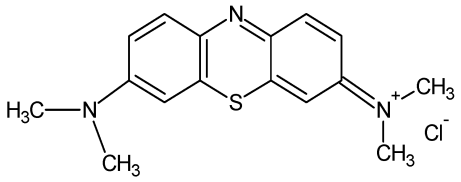

Figure 3.1: Chemical structure of methylene blue

Many techniques have been tested for dye removal and adsorption is considered the most efficient process due to its low cost, simplicity and lack of formation of harmful byproducts (Bulut and Aydin, 2006; Novais et al., 2018b; Rafatullah et al., 2010). Ion exchange is also commonly used in wastewater treatment (Cobzaru and Inglezakis, 2015; Wankat, 2012). Activated carbons are used as adsorbents due to their efficiency in dye removal. However, their high production cost urges the research on alternative economical and renewable adsorbents (Bergaoui et al., 2018; Mitrogiannis et al., 2015; Rafatullah et al., 2010).

Cellulose is the most abundant organic material in nature. It is biodegradable and renewable. Cellulose-based materials are commonly used in various applications, namely as adsorbents in wastewater treatment (Klemm et al., 2005; Vilela et al., 2010; Yan et al., 2011). The development of new cellulose-based polymers is motivated by the demand of low-cost and environmentally-friendly materials (Klemm et al., 2005).

Dicarboxymethyl cellulose (DCMC) is prepared by reaction of sodium 2-bromomalonate with cellulose (Chagas et al., 2019; Ferreira et al., 2019). Malonic acid has pK_a values of approximately 2.85 and 5.70, which the cellulose bond shouldn't greatly influence, resulting in deprotonated acid groups for pH greater than 3 (Kirk-Othmer, 2005). For this reason, DCMC can perform ion exchange at low pH (Chagas et al., 2019; Diamantoglou et al., 1977). The polymer works as a anionic polyelectrolyte, suitable for the removal of

positively charged synthetic dyes due to its active functional groups, such as hydroxyl and carboxyl (Diamantoglou et al., 1977; Ren et al., 2016). The use of a biodegradable source material facilitates its disposal (Chagas et al., 2019).

In this work, the potential of dicarboxymethyl cellulose for removal of methylene blue as a cationic dye model was investigated. Influence of parameters such as solution pH and number of carboxylate groups per grams of polymer was studied. Adsorption equilibrium and kinetic studies were performed. Equilibrium adsorption isotherms are essential in understanding the interactions between adsorbent and adsorbates, providing information on surface properties and adsorption capacities (Aquino et al., 2003; Bergaoui et al., 2018; Bulut and Aydin, 2006; Cao et al., 2018; Ren et al., 2018). Langmuir isotherm assumes adsorption occurs without lateral interactions between adsorbed molecules, producing homogeneous binding sites and a monolayer coverage of the outer surface of the adsorbent (Bergaoui et al., 2018; Novais et al., 2018a; Saber-Samandari et al., 2016). Freundlich isotherm states that adsorption occurs on an heterogeneous surface, where binding strength decreases with increasing occupation (Bergaoui et al., 2018; Novais et al., 2018a). Sips isotherm is a combination of the Langmuir and Freundlich isotherm models (Lima et al., 2015; Volesky, 2003). The Sips model indicates a multilayer adsorption at lower concentration and monolayer at higher concentration (Anirudhan et al., 2011; Lima et al., 2015). Kinetic studies give better understanding of the adsorption process, namely adsorbent behaviour in the presence of distinct adsorbates (Largitte and Pasquier, 2016; Liu et al., 2018; Ren et al., 2018). Lagergren first described adsorption kinetics of liquid-solid systems based on solid capacity (Febrianto et al., 2009; Ho, 2004). Lagergren's pseudo first-order (PFO) equation is based on the assumption of physisorption process Singha and Das, 2013. The PFO model assumes that the sorption rate decreases linearly as the sorption capacity increases (Yan et al., 2011). The pseudo second-order (PSO) model is similar to PFO, but it suggests a chemisorption process (Senthil Kumar et al., 2010; Singha and Das, 2013). Furthermore, adsorption coupled with filtration using a 500 kDa regenerated cellulose membrane and reusability studies were performed.

3.3 Materials and Methods

3.3.1 Materials

The polymers used are the ones whose synthesis and characterization is presented in Chapter 2 of this thesis. All reagents were used without further purification.

A standard citrate solution (25 mM, pH = 3) was prepared with sodium citrate dihydrate (MW = 294 g/mol) and citric acid monohydrate (MW = 210 g/mol) to be used as a buffer.

Deionized water was used to prepare methylene blue solutions with pH = 6.4.

Separate stock solutions with a concentration of 2 and 3 g/L were prepared by dissolving the required amount of methylene blue in deionized water and citrate buffer. The

solutions were diluted with the respective solvent to achieve the concentrations needed for the experiment, depending on the required pH.

3.3.2 Methods

3.3.2.1 Adsorption experiments of methylene blue

The influence of number of carboxylate groups per grams of polymer was studied at pH = 3. The process was also studied at pH = 6.4 (DI water) for the polymer with higher adsorption capacity. 2 mL of methylene blue solutions with concentrations between 40 and 3 000 mg/L were added to 4 mg of polymer and kept in a water bath for 48 h and at room temperature (25 °C). A Spectronic Helios Alpha spectrometer was used to determine methylene blue concentrations at 664 nm, by comparison with a calibration curve in the range of 0 to 4 mg/L prepared with methylene blue and deionized water or citrate buffer. The experiment was performed in triplicate and mean values were presented. The adsorption capacity is calculated by Equation (3.1).

$$q = \frac{(C_0 - C_e)\ V}{m} \tag{3.1}$$

where q (mg/g) is adsorption capacity; C_0 and C_e (mg/L) are the initial and equilibrium concentrations of methylene blue in the solution, respectively; V (L) is solution volume and m (g) is adsorbent mass.

3.3.2.2 Modelling of adsorption isotherms

Adsorption isotherms describe interactions between adsorbate and adsorbent (Saber-Samandari et al., 2016). In the present work, Langmuir, Freundlich and Sips models were used for analysis of equilibrium adsorption of methylene blue onto dicarboxymethyl cellulose.

The Langmuir isotherm is expressed by Equation (3.2) (Bergaoui et al., 2018; Novais et al., 2018a).

$$q = \frac{q_m\, C_e}{K_d + C_e} \tag{3.2}$$

where q_m (mg/g) is the maximum adsorption capacity, C_e (mg/L) is equilibrium concentration and K_d (L/g) is the Langmuir adsorption equilibrium constant, representing the affinity between adsorbate and binding sites.

The Freundlich mathematical model is expressed by Equation (3.3) (Bergaoui et al., 2018; Novais et al., 2018a).

$$q = K\, C_e^{\,1/n} \tag{3.3}$$

where K (L/g) is the Freundlich constant, which relates to adsorption capacity, C_e (mg/L) is equilibrium concentration and n is the heterogeneity factor. If n is equal to 1, all surface sites are equivalent and adsorption is linear. Larger values of n indicate strong

adsorbate-adsorbent interaction and it is generally stated that values of n in the range of 1 to 10 represent favourable adsorption (Febrianto et al., 2009).

The Sips equation is given by (Abramian and El-Rassy, 2009; Anirudhan et al., 2011; Lima et al., 2015; Senthil Kumar et al., 2010; Volesky, 2003):

$$q = \frac{q_m \; K_s C_e^{\,1/n_s}}{1 + \; K_s C_e^{\,1/n_s}} \tag{3.4}$$

where q_m (mg/g) is maximum adsorption capacity, C_e (mg/L) is equilibrium concentration, K_s (mg/L)$^{-1/n}$ is the Sips equilibrium constant and $1/n_s$ is the heterogeneity factor.

3.3.2.3 Kinetic adsorption experiments and modelling

Experiments were performed with 2 mL methylene blue solutions with concentrations of 4 and 40 mg/L, at pH = 3.0 and 6.4. Dicarboxymethyl cellulose dosage was varied to determine influence on methylene blue removal in a short period of time. The pseudo first-order and pseudo second-order non-linear kinetic models were used to fit the experimental data.

Pseudo first-order model is expressed by Equation (3.5) (Berizi et al., 2016; Largitte and Pasquier, 2016).

$$q = q_m \left(1 - e^{-K_1 t}\right) \tag{3.5}$$

where q_m (mg/g) is maximum adsorption capacity, K_1 (min^{-1}) is the rate constant and t (min) is time.

The Pseudo second-order model follows Equation (3.6) (Berizi et al., 2016; Largitte and Pasquier, 2016):

$$q = \frac{q_m^2 \, K_2 \, t}{1 + q_m \, K_2 \, t} \tag{3.6}$$

where q_m (mg/g) is maximum adsorption capacity, K_2 (mg g^{-1} min^{-1}) is the rate constant and t (min) is time.

3.3.2.4 Regenerability and reusability studies

Two experiments were performed where 100 mL of a 4 mg/L methylene solution was added to 200 mg of polymer. After three hours, the solution was decanted. NaCl 1M was used as an eluent for the desorption of dye molecules.

The first experiment was carried out through three cycles and the polymer was dried in a muffle furnace at 70 °C between the adsorption and desorption processes. In the second experiment, the polymer was washed with deionized water and decanted between adsorption and desorption. This reusability study was conducted through four cycles. Reusability of the polymer is determined by monitoring removal efficiency throughout the consecutive cycles. Adsorption and desorption efficiency are calculated by the following equations.

$$\text{Adsorption efficiency (\%)} = \frac{(C_0 - C_e)}{C_0} \cdot 100 \tag{3.7}$$

where C_0 and C_e (mg/L) are the initial and equilibrium concentrations of methylene blue in the solution, respectively.

$$\text{Desorption efficiency (\%)} = \frac{C_d}{(C_0 - C_e)} \cdot 100 \tag{3.8}$$

where C_d is the desorbed concentration of methylene blue and C_0 and C_e (mg/L) are the initial and equilibrium concentrations of methylene blue in the solution, respectively.

3.3.2.5 Adsorption coupled with filtration

An adsorption and filtration experiment under constant pressure mode was performed using the Membrane Extraction Technology (MET) cell system. Figure 3.2 presents the schematic diagram of the experimental setup.

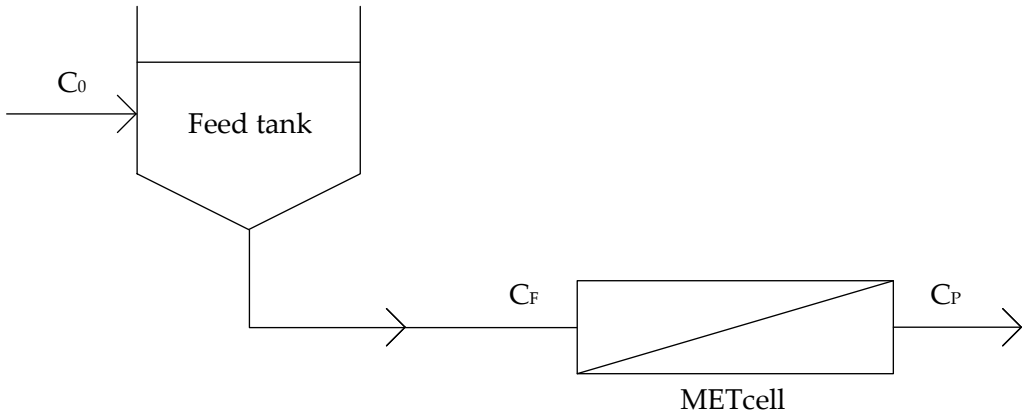

Figure 3.2: Schematic diagram of METcell filtration system

400 mg of DCMC 3 were added to 200 mL of a 4 mg/L methylene blue solution. The adsorption process was conducted at room temperature and pH = 6.4. After 30 min, the mixture was added to the MET cell system. An ultrafiltration membrane (Microdyn Nadir UC500) composed of regenerated cellulose with a molecular weight cut-off of 500 kDa was placed at the bottom of the MET cell and supported by a porous stainless steel disk. The system was operated under argon pressure of 5 bar. Feed and permeate samples were collected at predefined times for analysis of methylene blue concentration.

3.4 Results and Discussion

3.4.1 Adsorption isotherms

3.4.1.1 Effect of number of carboxylate groups

Adsorption experiments were carried out with the polymer with different number of carboxylate groups (CG) per grams of DCMC at pH = 3. Accordingly, Figure 3.3 shows that

maximum adsorption capacity increases linearly with the number of carboxylate groups per grams of polymer. A higher number of CG results in additional negatively charged functional groups, increasing the number of binding sites with affinity for positively charged proteins, such as methylene blue (Varshney and Naithani, 2011).

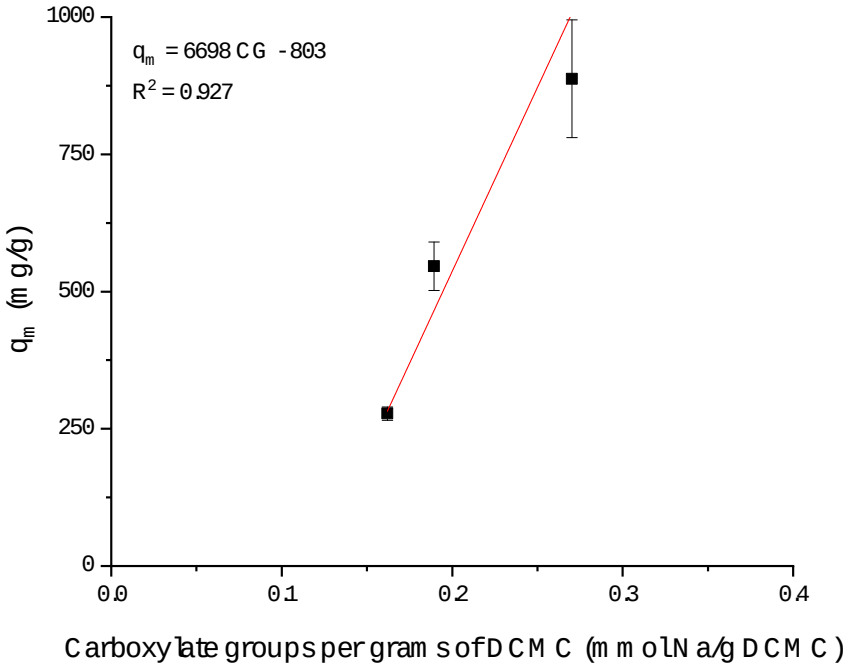

Figure 3.3: Effect of number of carboxylate units per grams of DCMC on maximum adsorption capacity.

Figure 3.4 illustrates the effect of number of carboxylate groups per grams of DCMC on adsorption isotherms at pH = 3. Adsorption capacity increases with increasing methylene blue concentration. Experimental data indicates that a plateau is reached with higher MB concentrations, suggesting a saturation point where no further adsorption can occur. Table 3.1 presents adsorption isotherm parameters calculated with fitting of Langmuir ($q = \frac{q_m C_e}{K_d + C_e}$) and Freundlich ($q = K\ C_e^{1/n}$) models. Based on the correlation coefficient values (R^2) presented in Table 3.1, Langmuir model offers a better description of the data. The R^2 obtained from the Freundlich model are 0.841, 0.789 and 0.767 for DCMC 1, DCMC 2 and DCMC 3 at pH = 3, respectively. Using the Langmuir isotherm model, correlation values were much higher ($R^2 > 0.9$). The applicability of the Langmuir model is consistent with the plateaus observed in Figure 3.4, indicating a monolayer adsorption process without lateral interactions between adsorbed molecules (Ren et al., 2018). The Langmuir model is often applied to ion exchange isotherms (Wankat, 1990). Maximum adsorption capacities calculated from the Langmuir model reached 277.6, 546.2 and 887.6 mg/g for DCMC 1, DCMC 2 and DCMC 3 at pH = 3, respectively (see Table 3.1). These values were all close to the experimental values, reinforcing the Langmuir model as an applicable fitting model.

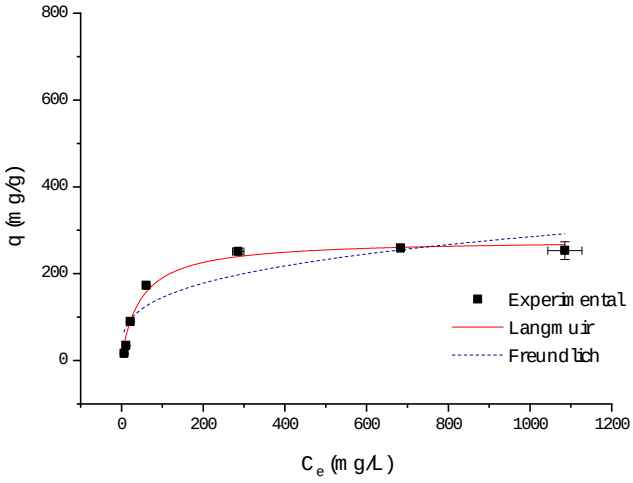

(a)

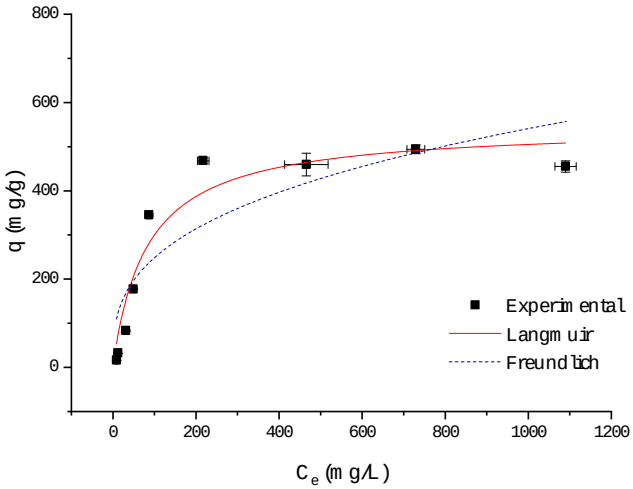

(b)

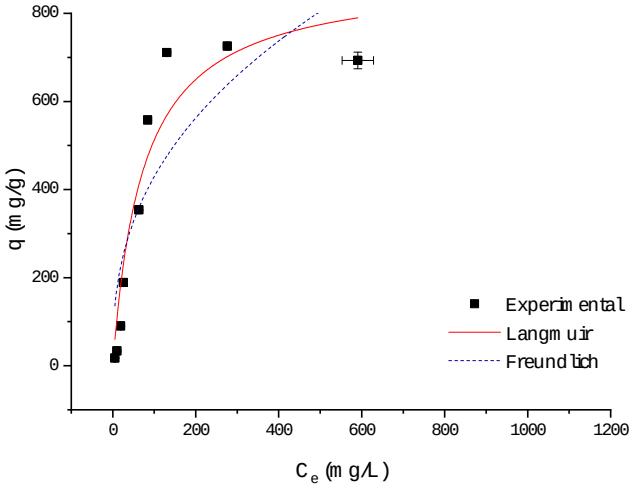

(c)

Figure 3.4: Adsorption isotherm at pH = 3 for a) DCMC 1, b) DCMC 2 and c) DCMC 3

Table 3.1: Adsorption isotherms parameters

		Langmuir			Freundlich		
Samples	pH	q_m (mg/g)	K_D (L/mg)	R^2	n	K (L/mg)	R^2
DCMC 1	3.0	277.6±12.0	0.021±0.004	0.913	3.4±0.9	0.037±0.018	0.841
DCMC 2		546.2±44.2	0.012±0.004	0.938	3.0±0.8	0.052±0.029	0.789
DCMC 3		887.6±107.4	0.014±0.005	0.921	2.6±0.7	0.071±0.040	0.767

3.4.1.2 Effect of pH

The pH of the dye solution is an important factor on the adsorption process, influencing the surface charge of the adsorbent, which consequently affects adsorption capacity (Anirudhan and Sreekumari, 2010; Khodaie et al., 2013). DCMC 3 provided better results for the adsorption experiment at pH 3, compared with the other samples. In order to investigate the effect of pH on methylene blue uptake, similar experiments were performed at pH = 6.4 with DCMC 3.

Figure 3.5 is characterized by S-shaped adsorption. These types of isotherms are usually associated with cooperation adsorption caused by solute-solute attraction and/or competing reaction with the solution, which inhibit solute adsorption (Inglezakis et al., 2018).

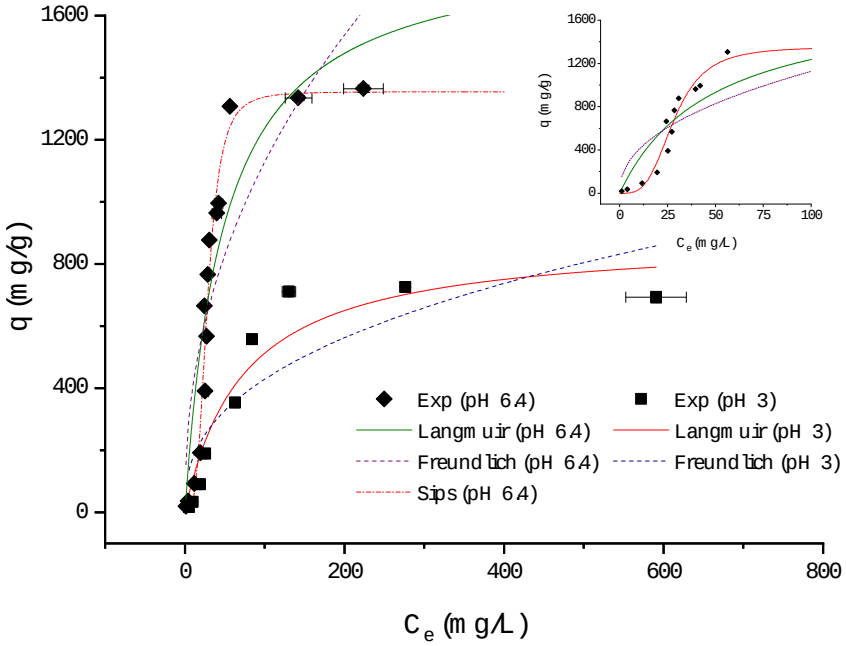

Figure 3.5: Effect of pH on adsorption isotherm of methylene blue in DCMC 3

From Figure 3.5 it is clear that maximum removal of methylene blue is achieved at pH = 6.4. With increasing pH, negatively charged binding sites increase and positively charged binding sites decrease, favoring adsorption of cationic dyes, such as methylene

blue. Conversely, at pH = 3.0 dicarboxymethyl cellulose has an increase in H^+ ion concentration resulting in electrostatic repulsion between the polymer and the cationic dye.

Since experimental data at pH = 6.4 did not adjust well to Langmuir and Freundlich model, the results were fitted with Sips ($q = \frac{q_m K_s C_e^{1/n_s}}{1+K_s C_e^{1/n_s}}$) model, a combination between the previous models (Hamdaoui and Naffrechoux, 2007). Based on the correlation factor ($R^2 = 0.968$), Sips described experimental data more appropriately. The calculated Sips heterogeneity factor n is 0.3 and equilibrium constant K_s is 8.794×10^{-6} $(mg/L)^{1/n}$. The calculated maximum adsorption capacity is very similar to the experimental value, 1354.6 and 1365.5 mg/g, respectively.

Figure 3.5 illustrates the effect of pH on adsorption isotherms of methylene blue onto dicarboxymethyl cellulose. As seen from the figure, adsorption rate and adsorption capacity at pH = 6.4 were significantly higher than at pH = 3.0. Maximum adsorption capacities for the best fitting models went from to 887.6 to 1354.6 mg/g for pH = 3.0 and 6.4, respectively. As mentioned previously, higher methylene blue uptake for higher pH is expected due to the increasing availability of binding sites.

3.4.1.3 Comparison with other adsorbents

Comparison of methylene blue adsorption on other adsorbents reported in literature is presented in Table 3.2. Adsorption capacity of dicarboxymethyl cellulose was higher than those found in literature, confirming that this novel cellulose-based adsorbent has potential for binding methylene blue from aqueous solutions.

Table 3.2: Comparison of maximum adsorption capacity of methylene blue with other adsorbents

Adsorbent	q_m (mg/g)	pH	Reference
DCMC	1354.6	6.4	Present study
MCA–E0.7/CMC [a]	998.2	7.0	Lin et al., 2017
CAC [b]	980.3	7.4	Kannan and Sundaram, 2001
A. platensis biomass [c]	312.5	7.5	Mitrogiannis et al., 2015
SCSM [d]	178.6	7.0	Zhao and Zhou, 2016
KT3B [e]	99.9	9.0	Mouni et al., 2018
DCMC	887.6	3.0	Present study
CHACZ [f]	463.0	4.0	Khodaie et al., 2013

[a] Epichlorohydrin-crosslinked carboxymethyl cellulose microspheres treated with 0.7 mL C_4H_9OH and modified with monochloroacetic acid
[b] Commercial activated carbon
[c] Arthrospira platensis biomass
[d] Extraction residues of Salvia mitiorrziza Bge modificated with 1 M $NaCO_3$
[e] Natural raw (Algerian) kaolin
[f] Corn husk by ZnCl2 activation

Commercial activated carbon (CAC) is commonly used in wastewater treatment (Cecen and Aktas, 2011). CAC are effective adsorbents, but have high production and regeneration costs (Bergaoui et al., 2018; Mitrogiannis et al., 2015). Alternatively, DCMC

is synthesized from an abundant biodegradable source, resulting in an economical adsorbent with facile disposal (Chagas et al., 2019). Results showed that DCMC has adsorption capacities in the same order of magnitude as CACs. Therefore, dicarboxymethyl cellulose may be used as a water remediation tool, namely in the removal of methylene blue from aqueous solutions.

3.4.2 Adsorption kinetics

Kinetic studies were performed at pH = 3.0 and 6.4, with initial concentrations of 4 and 40 mg/L. Changes in solution concentration over a period of time can be observed in Figures 3.6a, 3.7a, 3.8a and 3.9a. Results show that adsorption is almost instantaneous.

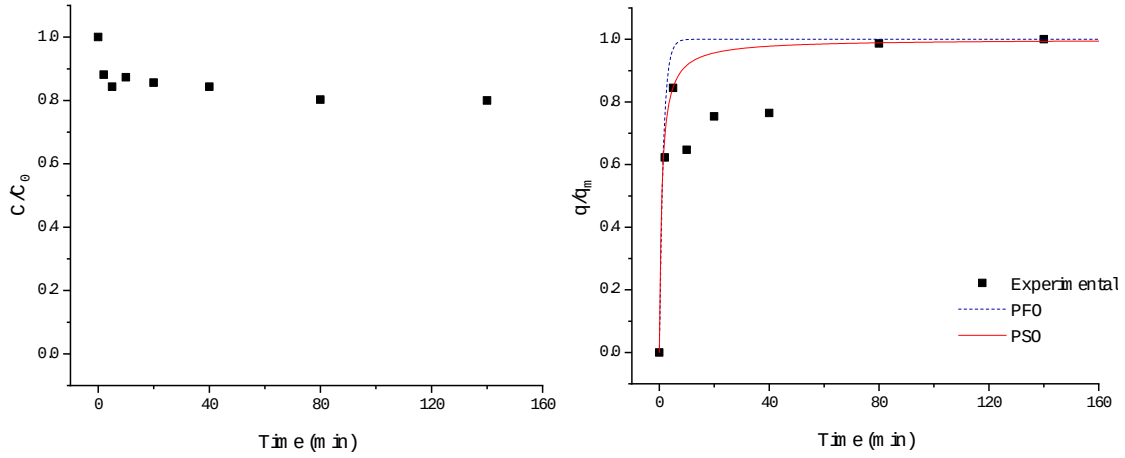

(a) (b)

Figure 3.6: Adsorption kinetics of a 4 mg/L solution at pH = 3.0 represented by normalized a) concentration and b) adsorption capacity.

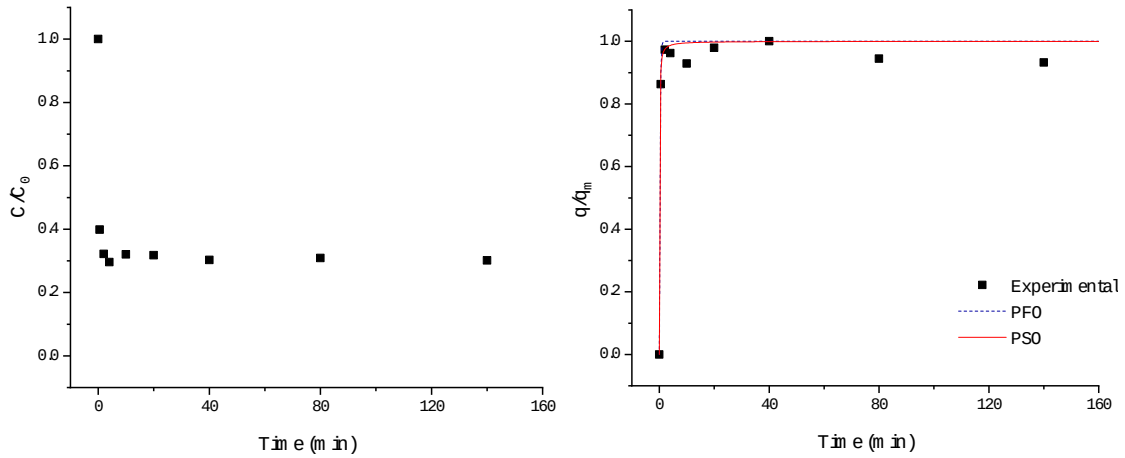

(a) (b)

Figure 3.7: Adsorption kinetics of a 4 mg/L solution at pH = 6.4 represented by normalized a) concentration and b) adsorption capacity.

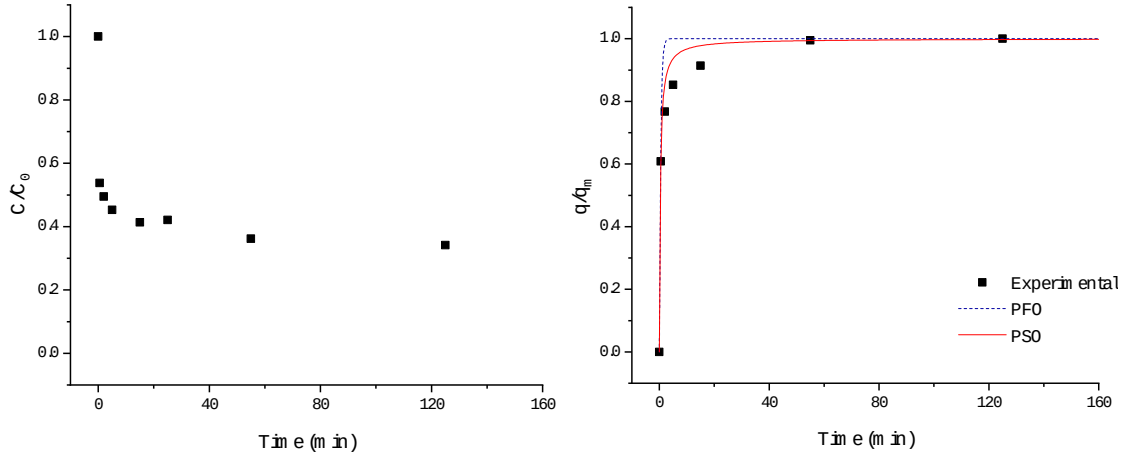

(a) (b)

Figure 3.8: Adsorption kinetics of a 40 mg/L solution at pH = 3.0 represented by normalized a) concentration and b) adsorption capacity.

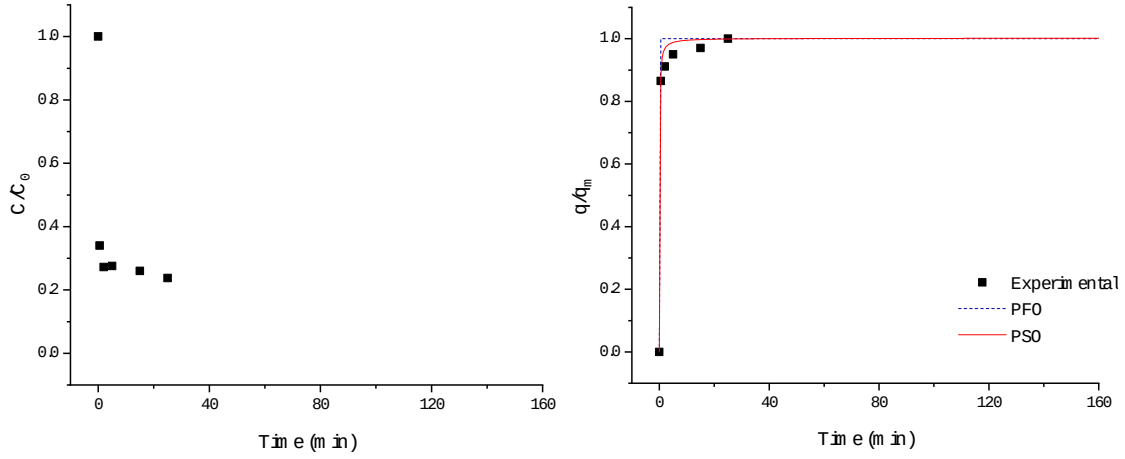

(a) (b)

Figure 3.9: Adsorption kinetics of a 40 mg/L solution at pH = 6.4 represented by normalized a) concentration and b) adsorption capacity.

Figures 3.6 to 3.9 show the effect of pH and influence of initial dye concentration in methylene blue adsorption kinetics at 4 and 40 mg/L initial concentration. For the same concentration, an increase in pH results in a higher dye uptake, consistent with the results on Section 3.4.1.

Adsorption capacity of methylene blue was calculated by $q = \frac{(C_0 - C_e)\,V}{m}$. As shown in Figures 3.6 to 3.9, the adsorption of methylene blue onto DCMC was very rapid. There is almost complete dye removal in the first five minutes. After this rapid adsorption an equilibrium is established. Adsorption capacities obtained for 40 mg/L of initial methylene blue concentration, represented in Figures 3.8 and 3.9, were in agreement with the results obtained in Section 3.4.1.

Experimental data on the adsorption of methylene blue onto dicarboxymethyl cellulose was adjusted to pseudo first-order ($q = q_m \left(1 - e^{-K_1 t}\right)$) and pseudo second-order ($q = \frac{q_m^2 K_2 t}{1 + q_m K_2 t}$) kinetic models. The adsorption kinetic parameters are displayed in Table 3.3. The data shows high correlation factors (R^2) for both kinetic models at pH = 6.4. However, at pH = 3 the experimental data is better adjusted by pseudo second-order model. Calculated adsorption capacity values from PSO are close to experimental results, suggesting the applicability of this model for methylene blue adsorption kinetics on dicarboxymethyl cellulose.

Table 3.3: Adsorption kinetics parameters

		Pseudo first order			Pseudo second order		
pH	C (mg/L)	K_1 (min $^{-1}$)	q_m (mg/g)	R^2	K_2 (mg g^{-1} min^{-1})	q_m (mg/g)	R^2
3.0	4	0.699±0.324	0.835±0.055	0.860	1.252±0.861	0.881±0.062	0.883
	40	2.044±0.539	12.646±0.536	0.952	0.221±0.048	13.285±0.339	0.986
6.4	4	4.587±0.534	3.116±0.030	0.995	6.014±2.204	3.134±0.037	0.993
	40	43.246±3.340	50.346±1.450	0.985	0.276±0.072	52.676±0.691	0.997

From Table 3.3, it can be observed that the adsorption capacity increases with the increase of methylene blue concentration and increasing pH. As the initial dye increases the adsorption capacity of methylene blue onto the polymer changes from 0.881 to 13.285 mg/g, at pH = 3.0, and 3.134 to 52.676 mg/g, at pH = 6.4. Also, the kinetic rate constant K_2 decreases with increasing methylene blue concentration. When dye concentration is higher, competition for binding sites on the polymer's surface increases, lowering the kinetic rates.

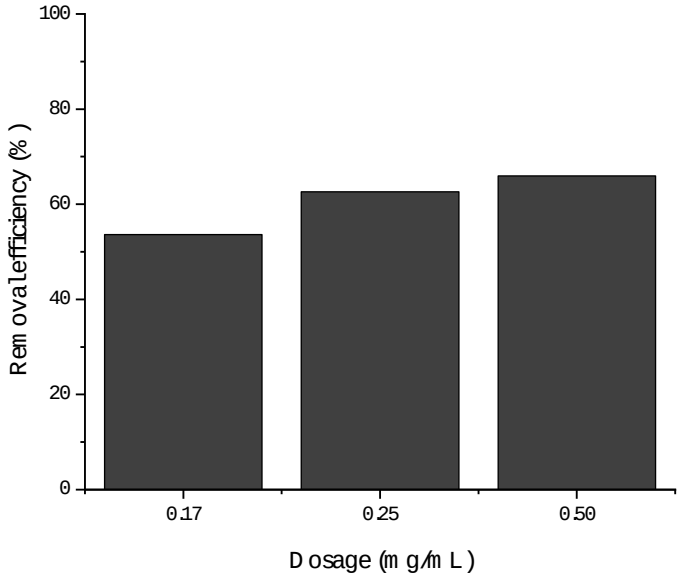

Figure 3.10: Effect of DCMC dosage on methylene blue removal after 30 seconds

Since the adsorption process is almost instantaneous, the ratio between polymer mass

and the solution volume, denominated as dosage, was varied. Figure 3.10 shows that evolution of the adsorption kinetic process with 40 mg/L initial concentration at pH = 6.4. In order to observe a continuous decrease of methylene blue concentration, dosages were reduced up to 0.17 mg/mL and samples were taken at 30 seconds. Nonetheless, the adsorption process is very quick, achieving 50% methylene blue removal in only 30 seconds. This suggests smaller doses of polymer may be used depending on the desired final concentrations and on the imposed timetable.

3.4.3 Reusability study

The regenerability of an adsorbent is an important aspect, particularly with the increasing environmental awareness. To study the reusability of dicarboxymethyl cellulose, 1 M NaCl was used as an eluent in two different experiments.

In the first experiment, the polymer was dried in a muffle furnace between adsorption and desorption cycles. Figure 3.11 shows that desorption efficiency remained relatively constant throughout the cycles. However, adsorption capacity decreased significantly after the second cycle. Between adsorption and desorption processes, the polymer was dried in a muffle furnace at 70 °C. Cross-linking occurs at 90-100 °C, so it is possible that the polymer may have continued to cross-link. Since the carboxylic groups are involved in the cross-linking reaction, a reduction of active binding sites may justify the loss in adsorption capacity. Also, temperature-induced decarboxylation may have produced carboxymethylcellulose (CMC). CMC has a higher pKa than DCMC (4.5 versus 2.1, respectively). For this reason, CMC has a smaller pH range where ionized groups are able to interact with cationic compounds resulting in reduced adsorption capacity (Wuestenberg, 2014).

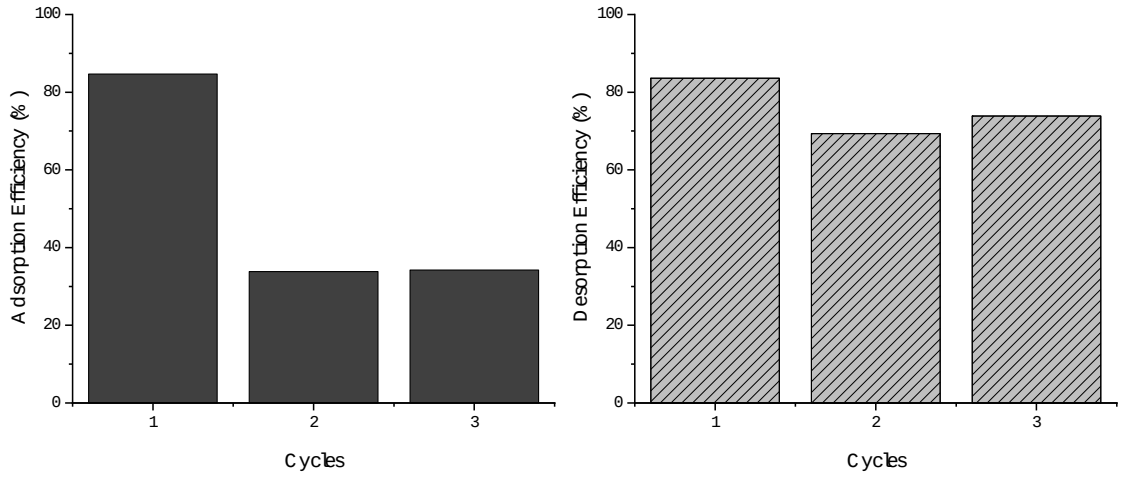

(a) (b)

Figure 3.11: Removal efficiency for different adsorption-desorption cycles with in-between drying (adsorbent dosage: 2 mg/mL, pH = 6.4) represented by a) adsorption and b) desorption efficiency.

Figure 3.12 represents the second reusability experiment where the polymer was not dried. It is clear that after several consecutive cycles, adsorption and desorption efficiency decreased. The effect on adsorption performance may be justified by the presence of dye on the adsorbent surface. The presence of residual cationic dye in the adsorbent may also contribute to an increase of electrostatic repulsion, preventing other dye molecules from occupying free adsorption binding sites. Moreover, desorption efficiency strongly decreased after the consecutive cycles. This indicates that the electrostatic attraction between the cationic dye and the negative surface charge of the polymer wasn't significantly reduced, hindering the desorption process.

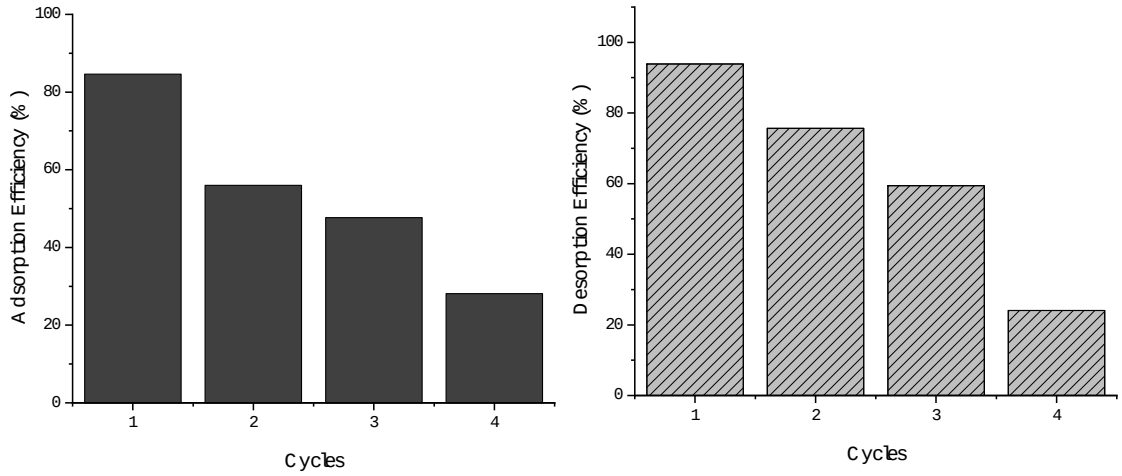

(a) (b)

Figure 3.12: Removal efficiency for different adsorption-desorption cycles (adsorbent dosage: 2 mg/mL, pH = 6.4) represented by a) adsorption and b) desorption efficiency.

For future work, experiments on reusability should consider product filtration in order to remove non-adsorbed dye molecules present in the solution. As desorption efficiency also decreased throughout the cycles, desorption studies as a function of desorbing agents should be carried out. By increasing ionic strength, electrostatic attraction between positively-charged molecules and the surface of the polymer is reduced (Li et al., 2012). Therefore, using stronger eluent agents, such as 2 M NaCl or HCl, may increase desorption.

3.4.4 Adsorption coupled with filtration

In this experiment, 200 mL of a methylene blue solution (C_0) were added to 400 mg of polymer. After 30 minutes, the polymer had removed 77.4% of the cationic dye and the solution had a reduced concentration of 1.18 mg/L (C_F). A 500 kDa membrane was placed at the bottom of a METcell system and the solution was permeated by using a transmembrane pressure of 5 bar. The differences in solution concentration throughout this process are presented in Table 3.4.

Table 3.4: Results from the adsorption and filtration process

Sample	C (mg/L)	Removal Efficiency (%)
C_0	4.28	NA[a]
C_F	1.18	77.4
C_P	0.01	99.8

[a] Not applicable

After filtration with the MET cell system, the permeate was clear (see Figure 3.13). Analysis showed residual (less than 10 ppb) methylene blue concentration. The selected membrane has a pore size of 500 kDa whereas methylene blue has a molar mass of 319.85 Da, which suggests that dicarboxymethyl cellulose completely sequestered the cationic dye. Figure 3.14 shows the recovery of the retentate after filtration was complete.

Figure 3.13: Experimental setup for filtration using a MET cell system

The permeate fluxes generated during the course of the membrane filtration process are displayed in Figure 3.15. A continuous decrease in permeate flux is caused by membrane fouling, offering increasing resistance to the system.

In order to determine resistance, flux was calculated using a modified Darcy's law, represented in Equation (3.9). Total resistance includes membrane and polymer layer resistance. The process was carried out for 6153 seconds until the aqueous solution of methylene blue was completely filtrated. The viscosity of the aqueous solution was considered to be the viscosity of water at 20 °C.

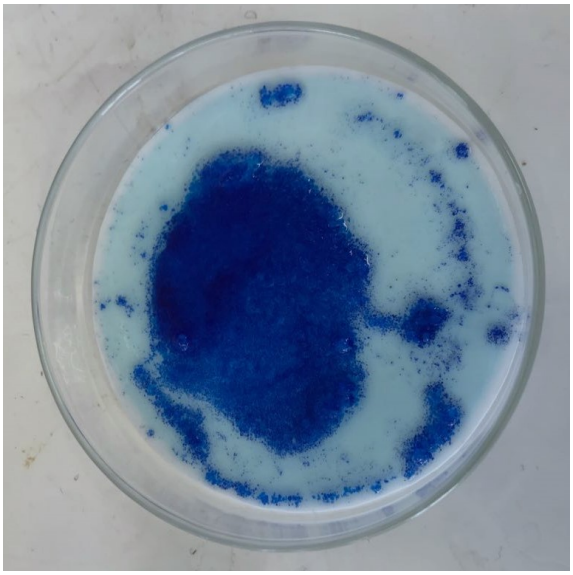

Figure 3.14: Retentate recovered from the filtration experiment: dicarboxymethyl cellulose loaded with methylene blue.

$$J = \frac{V}{A\,t} = \frac{\Delta P}{\mu R_T} \tag{3.9}$$

where J ($m^3/(m^2 \cdot s)$) is filtrate flux rate, V (m^3) is volume, A (m^2) is membrane area, t (s) process is time, ΔP (Pa) is transmembrane pressure, μ (mPa · s) is viscosity and R_T (m^{-1}) is total resistance.

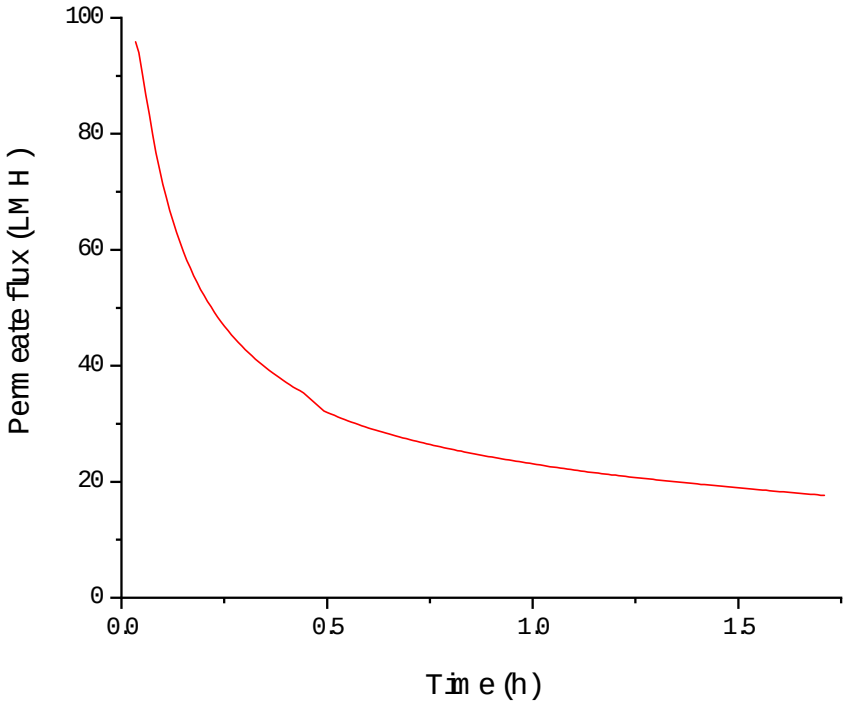

Figure 3.15: Permeate flux variation over time

Membrane resistance was calculated by performing the experiment with water. A flux of 2.57×10^{-4} $m^3/(m^2 \cdot s)$ was obtained. Using Equation (3.9) and substituting R_T by R_M a value of 1.94×10^{12} m^{-1} was obtained. Then, with the final experimental flux of 4.90×10^{-6} $m^3/(m^2 \cdot s)$, a total resistance of 1.02×10^{14} m^{-1} was determined by Equation (3.9). Polymer layer resistance was then calculated with Equation (3.10) and determined to be 1.00×10^{14} m^{-1}. Therefore, the dicarboxymethyl cellulose layer offers 98.1% resistance to the system. This high resistance can be decreased working on cross-flow mode instead of dead-end mode as described.

$$R_T = R_M + R_P \tag{3.10}$$

where R_T (m^{-1}) is total resistance, R_M (m^{-1}) is membrane resistance and R_P (m^{-1}) is polymer resistance.

3.5 Conclusions

In this study, dicarboxymethyl cellulose prepared from air-dry cellulose was used for the adsorption of methylene blue from aqueous solutions. Experimental results showed that methylene blue adsorption was dependent on adsorbent surface characteristics, which are manipulated by solution pH. At an acidic pH, Langmuir isotherm model adjusted better to experimental data, suggesting monolayer adsorption on a homogenous adsorbent surface. The maximum dye uptake at these conditions was 887.6 mg/g. At pH = 6.4, experimental data fitted with Sips isotherm model with calculated maximum adsorption capacities similar to experimental values (1354.6 and 1365.5 mg/g, respectively). High dye uptakes suggest dicarboxymethyl cellulose can be used as an alternative to commercial adsorbents. Kinetics studies revealed experiments were well described by pseudo second-order kinetic model which is associated with chemisorption processes. Methylene blue adsorption onto DCMC is almost instantaneous with more than 50% removal efficiency after 30 seconds. Reusability studies showed a decrease in desorption efficiency throughout consecutive cycles, which may have influenced the decrease in adsorption efficiency. Adsorption coupled with filtration was successful in the removal of methylene blue. Even though the membrane pore size was much larger than methylene blue, the molecule was not permeated. Therefore, methylene blue was completely sequestered by DCMC.

DCMC exhibited potential as an effluent treatment material. Moreover, the use of a low-cost, cellulose-based polymer offers promising benefits for commercial purposes. Nevertheless, future studies should include scale-up experiments with cost-benefit analysis to assess commercial viability of the polymer. Future work should also address the use DCMC in the treatment of real wastewaters. Further reusability studies should consider desorbing agents with higher ionic strength.

Chapter 4

Adsorption of Cytochrome *C*

4.1 Summary

In the present study, a novel cellulose-based polymer is used in protein adsorption. Dicarboxymethylcelllose (DCMC) was evaluated as a cytochrome *C* (Cyt *C*) adsorbent. Factors affecting the adsorption capacity of DCMC such as adsorbent dosage, number of carboxylate groups per gram of polymer and time were investigated. Removal efficiency increased with increasing adsorbent dosage, reaching a balanced value of approximately 90% at a critical dosage of 0.25 mg/mL. Cytochrome *C* uptake increased with number of carboxylate groups. The adsorption process followed the Langmuir adsorption isotherm, suggesting monolayer coverage. Maximum protein uptake was 1279.6 mg/g for the highest substituted polymer (DCMC 3). Pseudo second-order kinetic model adjusted well to experimental data. Selective adsorption experiments revealed that DCMC does not display preferential equilibrium uptake of Cyt *C* over lysozyme (Lys). Doping Cyt *C* with Lys in a competitive environment did not affect the uptake of Cyt *C*. Furthermore, DCMC was successfully regenerated and reused (up to 3 cycles) without compromising performance. After three cycles, adsorption efficiency was above 90%.

4.2 Introduction

Proteins are complex and sophisticated biomolecules that participate in several physiological processes (Alberts et al., 2002; Qiao et al., 2019). The increasing demand for proteins in research and other applications contributed to the scientific importance of the adsorption phenomenon applied to these biomolecules (Bellezza et al., 2009; Kondo and Higashitani, 1992).

Protein adsorption has been thoroughly studied throughout the years (Kondo and

Higashitani, 1992; Qiao et al., 2019). With the recent interests in green technology, the applications of the adsorption process have expanded (Tien, 2018). Adsorption is applied to the recovery and immobilization of proteins, namely for pharmaceutical and biomedical purposes (Anirudhan et al., 2011; Miyahara et al., 2007; Tien, 2018). Therefore, understanding the mechanisms of protein adsorption is vital to enhance the separation or removal efficiency of the proteins (Anirudhan et al., 2011; Bellezza et al., 2009). Adsorption is affected by chemical and physical characteristics of the protein and the adsorbent (Bellezza et al., 2009). Molecular size, surface charge, hydrophobicity and electrostatic interactions are some of the factors that influence adsorption behavior (Bellezza et al., 2009; Kondo and Higashitani, 1992).

The research and design of adsorbents with high adsorption capacities is of great importance (Qiao et al., 2019). Moreover, environmental awareness leads to a research on sustainable and renewable adsorbents (Liu et al., 2018). Cellulose is the most abundant organic material on Earth with 1.5 x 10^{12} tons of annual production (Kirk-Othmer, 2005; Klemm et al., 2005). This raw material is biodegradable, renewable and a potential adsorbent (Klemm et al., 2005; Suhas et al., 2016). However, naturally occurring cellulose has low protein adsorption capacity as well as variable physical stability (Anirudhan et al., 2011; Suhas et al., 2016). Therefore, derivatization of cellulose is necessary to introduce new physical and chemical properties (Xiao et al., 2014). Through functionalization of cellulose, a novel polymer was synthesized. Dicarboxymethyl cellulose is prepared by heterogenous etherification with bromomalonic acid (Chagas et al., 2019; Diamantoglou et al., 1977; Ferreira et al., 2019; Kötz et al., 1991). Due to the presence of a low pKa ether group, dicarboxymethyl cellulose can perform ion exchange at low pH (2.5 – 3.5) (Chagas et al., 2019).

Cytochrome *C* is a small heme protein (MW ≈ 13 kDa) with a high isoelectric point (pI = 10.0-10.5) (Anirudhan et al., 2011; *Sigma-Aldrich Product Information*; Vinu et al., 2004). Cyt *C* is well-characterized and often used as a model protein (Kondo and Higashitani, 1992; Takeda et al., 2015). The chemical structure of the protein is presented on Figure 4.1.

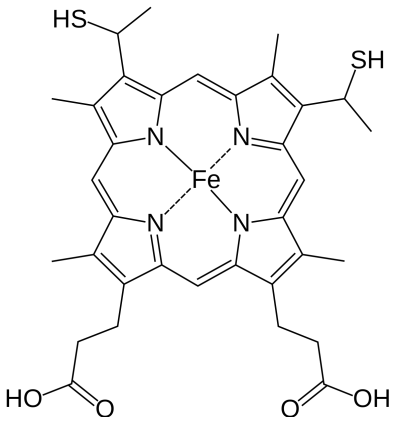

Figure 4.1: Chemical structure of cytochrome *C*

In the present contribution, the adsorption behavior of Cytochrome *C* onto dicarboxymethyl cellulose was studied. The cellulose-based polymer is prepared following the method described by Chagas et al., 2019; Ferreira et al., 2019. Adsorption isotherm and kinetics were studied. Effect of pH of the solution and degree of substitution of the adsorbent were considered. Reusability studies of the polymer were carried out. Furthermore, competitive and selective experiments using an analogous protein, lysozyme, were performed.

4.3 Materials and Methods

4.3.1 Materials

The polymers used are the ones whose synthesis and characterization is presented in Chapter 2 of this thesis. Horse heart cytochrome *C* (Cyt *C*, MW = 12.4 kDa, pI = 10.0-10.5) and Lysozyme (Lys, MW = 14.3 kDa, pI = 11.35) were purchased from Sigma-Aldrich. All other reagents were used without further purification.

A standard phosphate solution (25 mM, pH 7.2) was prepared with the required quantities of sodium phosphate dibasic heptahydrate (MW = 268 g/mol) and sodium phosphate monobasic dihydrate (MW = 156 g/mol).

4.3.2 Methods

4.3.2.1 Adsorption experiments for Cytochrome *C* removal

Experiments were carried out to determine the effect of number of carboxylate groups and adsorbent dosage on adsorption capacities.

Adsorption isotherms were studied at pH 7.2 with sodium phosphate buffer. 200 mg/L cytochrome *C* solutions were added to the polymers in adsorbent dosages between 0.06 and 2.00 mg/mL. The vials were stirred continuously on a multi-mixer for 48 h. A Spectronic Helios Alpha spectrometer was used to determine cytochrome *C* concentrations at 409 nm. All experiments were performed in triplicate and mean values were presented.

4.3.2.2 Modelling of adsorption isotherms

The adsorption isotherms of Cytochrome *C* onto DCMC were studied by fitting the experimental data with known mathematical models. The theoretical reasoning behind this study is described in detail in Chapter 3. Langmuir and Freundlich models were used to describe the data.

The Langmuir isotherm model is expressed by Equation (4.1).

$$q = \frac{q_m C_e}{K_d + C_e} \tag{4.1}$$

where q_m (mg/g) is the maximum adsorption capacity, C_e (mg/L) is equilibrium concentration and K_d (L/g) is the Langmuir adsorption equilibrium constant, representing the affinity between adsorbate and binding sites.

The Freundlich isotherm model follows Equation (4.2).

$$q = K\, C_e^{1/n} \tag{4.2}$$

where K (L/g) is the Freundlich constant, which relates to adsorption capacity, C_e (mg/L) is equilibrium concentration and n is the heterogeneity factor. If n is equal to 1, all surface sites are equivalent and adsorption is linear. Larger values of n indicate strong adsorbate-adsorbent interaction and it is generally stated that values of n in the range of 1 to 10 represent favorable adsorption (Febrianto et al., 2009).

4.3.2.3 Modelling of adsorption kinetics

In this experiment, 200 mL of a 20 mg/L Cytochrome *C* solution were added to 200 mg of DCMC 3. Experimental data was fitted with two non-linear kinetic models, thoroughly described in Chapter 3.

The pseudo first-order kinetic model is calculated by Equation (4.3) (Largitte and Pasquier, 2016; Liu et al., 2018; Ren et al., 2018).

$$q = q_m \left(1 - e^{-K_1 t}\right) \tag{4.3}$$

where q_m (mg/g) is maximum adsorption capacity, K_1 (min^{-1}) is the rate constant and t (min) is time.

Pseudo second-order follows Equation (4.4) (Berizi et al., 2016; Largitte and Pasquier, 2016).

$$q = \frac{q_m^2\, K_2\, t}{1 + q_m\, K_2\, t} \tag{4.4}$$

where q_m (mg/g) is maximum adsorption capacity, K_2 (mg g^{-1} min^{-1}) is the rate constant and t (min) is time.

4.3.2.4 Reusability study

In this study, 6 mL of a 200 mg/L Cytochrome *C* solution were added to 6 mg of the polymer with a higher number of carboxylate groups (DCMC 3). After three hours, the solution was decanted, washed three times with deionized water and decanted once more. The same volume of 1 M NaCl was added to dicarboxymethyl cellulose in order to remove the protein by ionic exchange. Reusability of the polymer is determined by monitoring removal efficiency throughout the consecutive cycles. Adsorption and desorption efficiency are calculated by the following equations.

$$\text{Adsorption efficiency (\%)} = \frac{(C_0 - C_e)}{C_0} \cdot 100 \tag{4.5}$$

where C_0 and C_e (mg/L) are the initial and equilibrium concentrations of Cyt *C* in the solution, respectively.

$$\text{Desorption efficiency (\%)} = \frac{C_d}{(C_0 - C_e)} \cdot 100 \tag{4.6}$$

where C_d is the desorbed concentration of Cyt *C* and C_0 and C_e (mg/L) are the initial and equilibrium concentrations of Cyt *C* in the solution, respectively.

4.3.2.5 Competitive adsorption of cytochrome *C* and lysozyme

To determine selectivity of dicarboxymethyl cellulose for Cytochrome *C*, a model protein (Lysozyme) with similar characteristics was used.

Solutions of Cyt *C* and Lys were prepared with a concentration of 200 mg/L, using a phosphate buffer solution (pH = 7.2). Adsorption experiments for Cyt C and Lys were performed separately. Equilibrium concentration was determined by measuring UV absorbance after the mixtures were shaken for 48 h at room temperature.

The competitive adsorption experiment was studied by adding phosphate buffer solution (pH = 7.2) with cytochrome *C* and lysozyme in the same concentration (200 mg/L) to dicarboxymethyl cellulose. Identically to previous adsorption experiments, the mixture was stirred for 48 h at room temperature. Equilibrium concentrations for Cyt C and Lys were calculated by measuring UV absorbance at 409 and 280 nm, respectively.

4.4 Results and Discussion

4.4.1 Effect of DCMC dosage and number of carboxylate groups

The appearance of the samples before and after the adsorption experiments are shown in Figure 4.2. From the picture, it is evident that the polymer with a higher number of carboxylate groups (DCMC 3) has better results than the other polymers. Logically, the vials with clearer solutions are the ones where the polymer has a more intense reddish color. A decrease in the solution color intensity can be observed with increasing number of carboxylate functional groups. This can be explained by the availability of negatively-charged binding sites for cationic proteins. The removal of Cyt *C* originates a clear and colorless solution.

The effect of adsorbent dosage was studied on Cytochrome *C* removal. Figure 4.3 illustrates the influence of DCMC dosage on Cyt *C* removal efficiency. Results show that increasing adsorbent dosage beyond 0.25 mg/mL does not affect removal. At this critical dosage, removal efficiency reaches a balanced value of approximately 90%. For the same contact time, maximum removal of Cyt *C* reached 95% with a dosage of 2.00 mg/mL, while at 0.06 mg/mL there was 38% removal. These results can be explained by the increasing number of binding sites with increasing amount of adsorbent.

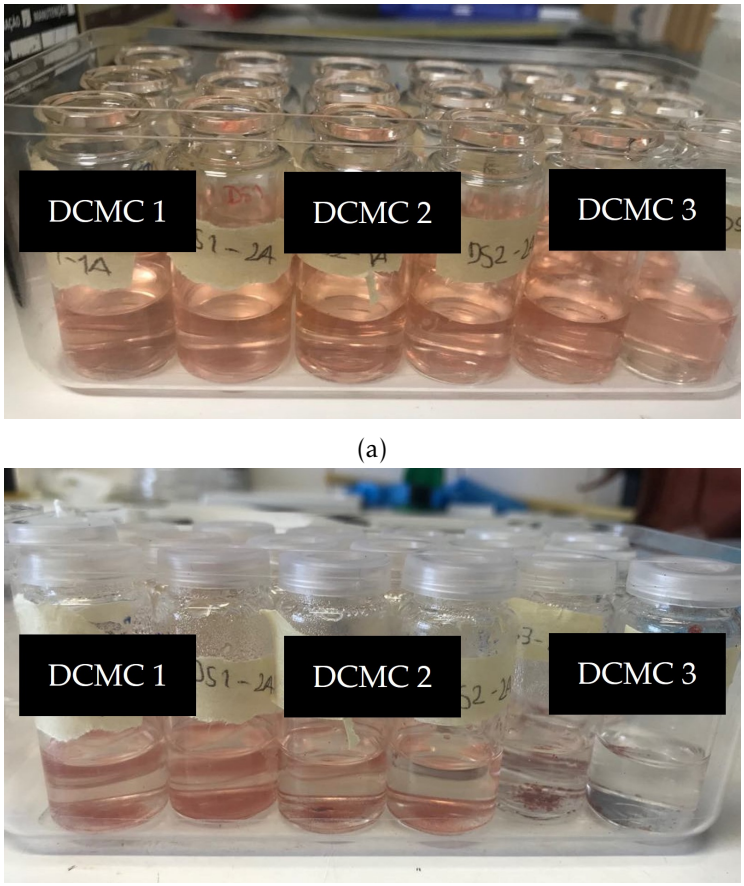

(a)

(b)

Figure 4.2: Pictures of the samples a) before and b) after the adsorption experiment of Cyt *C* onto DCMC.

At high dosages, the number of carboxylate groups (CG) per grams of polymer has no influence on the removal efficiency of Cytochrome *C*. However, at lower dosages removal efficiency increases with increasing CG. For the same DCMC dosage, an increase in CG results in increasing available binding sites which facilitates protein adsorption.

4.4.2 Adsorption isotherm

Based on the results obtained in the previous section, an adsorption isotherm experiment was conducted with the most efficient polymer, regardless of dosage. To understand the adsorption mechanism of Cytochrome C the experiment was conducted with the polymer with highest number of carboxylate groups (DCMC 3).

The experimental data was adjusted to Langmuir and Freundlich models. Table 4.1 presents the calculated adsorption isotherm parameters. Correlation coefficients (R^2) show that Langmuir model adjusts better to experimental data, compared to Freundlich model. Additionally, adsorption capacity calculated by the Langmuir model (q_m = 1279.6 mg/g) is in agreement with experimental results (q_m = 1142.8 mg/g). Fitting with

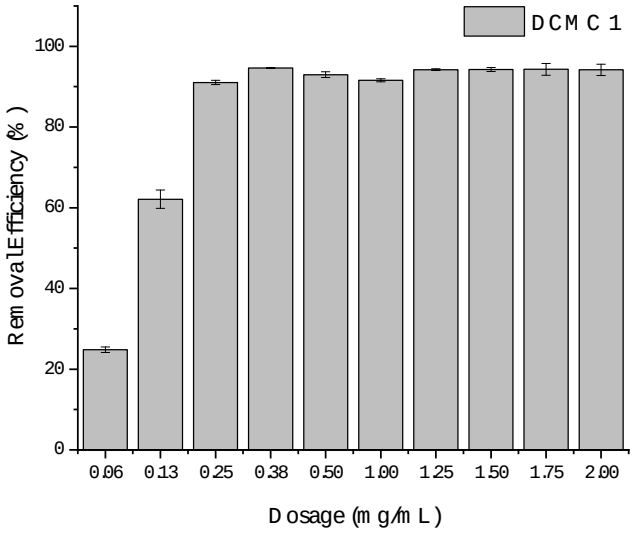

(a)

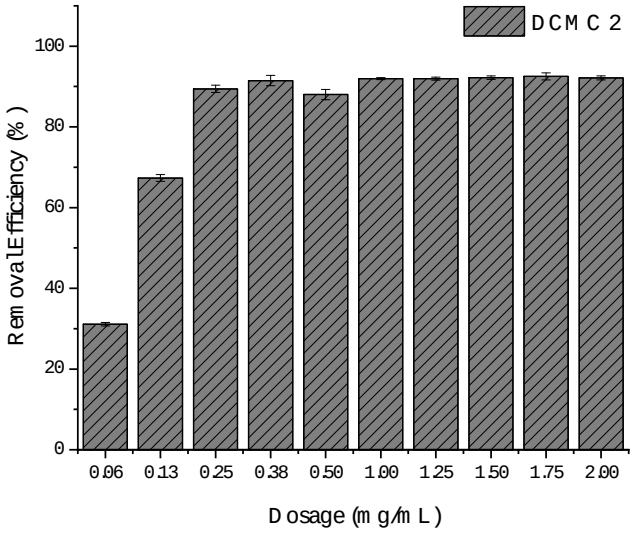

(b)

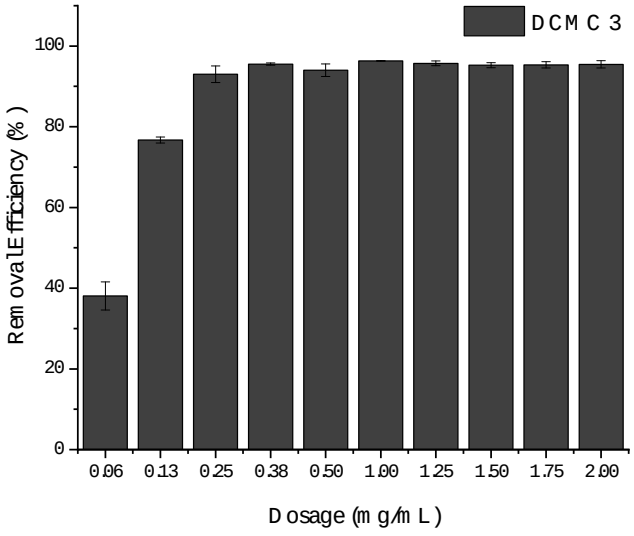

(c)

Figure 4.3: Effect of DCMC dosage on Cytochrome *C* removal efficiency for a) DCMC 1, b) DCMC 2 and c) DCMC 3 at pH 7.2.

Langmuir model suggests adsorption of Cyt C onto dicarboxymethyl cellulose is a monolayer process.

Table 4.1: Adsorption isotherm parameters

		Langmuir			Freundlich		
Sample	pH	q_m (mg/g)	K_D (L/mg)	R^2	n	K (L/mg)	R^2
DCMC 3	7.2	1279.6±95.6	0.095±0.026	0.947	4.2±1.5	0.385±0.127	0.823

4.4.3 Comparison with other adsorbents

Comparison of the adsorption capacity of Cytochrome *C* onto other adsorbents is presented in Table 4.2.

Adsorption capacity of DCMC3 was significantly higher than those reported in literature. Based on these results, it was found that dicarboxymethyl cellulose may be used for the removal of Cyt *C*.

Table 4.2: Comparison of maximum adsorption capacity of Cytochrome *C* with other adsorbents

Adsorbent	q_m (mg/g)	pH	Reference
DCMC	1279.6	7.2	Present study
MPSs [a]	453.3	5.0	Li et al., 2012
5 nm nanodiamonds	195.0	6.5	Huang and Chang, 2004
APSs [b]	180.8	5.0	Li et al., 2012
CPSs [c]	173.2	5.0	Li et al., 2012
MIMs [d]	156.1	7.4	Li et al., 2018
PSs [e]	101.2	5.0	Li et al., 2012
100 nm nanodiamonds	97.0	6.5	Huang and Chang, 2004
NIMs [f]	38.6	7.4	Li et al., 2018

[a] Modified peanut shells
[b] Alkaline peanut shells
[c] Crosslinked peanut shells
[d] Molecularly imprinted mesoporous materials
[e] Unmodified peanut shells
[f] Non-imprinted mesoporous materials

Several reports mention Ion Exchange Chromatography (IEC) as a method for protein separation (Bonner, 2007; Guthrie and Bullock, 1960; Peterson and Sober, 1956; Zeng and Ruckenstein, 1998). Carboxymethyl cellulose, diethylaminoethyl cellulose, quaternary aminoethyl cellulose, sulphopropyl cellulose and methyl sulphone cellulose are commercially available ion exchange resins (Zeng and Ruckenstein, 1998). These resins can be classified as cation or anion-exchangers, respectively attracting negative or positively-charged proteins (Bonner, 2007; Cobzaru and Inglezakis, 2015). Depending on the ionization range, ion exchange resins are considered weak or strong (Bonner,

2007). Strong ion exchange resins have wider working pH windows (Bonner, 2007). Dicarboxymethyl cellulose and carboxymethyl cellulose (CMC) are similar in structure, with the former having an additional carboxymethyl functional group. The potential of DCMC as a cation-exchanger resin is motivated by its similarities with CMC and wider pH range.

4.4.4 Adsorption kinetics

The kinetic experiment was performed on the polymer with higher number of carboxylate groups. A 20 mg/L Cytochrome *C* solution was added to 200 mg of DCMC 3. Figure 4.4 shows the adsorption kinetic process of Cytochrome *C* onto dicarboxymethyl cellulose.

Based on Figure 4.4a, Cyt *C* was rapidly removed in the first 100 min. In that period of time, concentration is reduced to a third of its initial value. Then, equilibrium concentration reaches a plateau which may be explained by the reduction of available binding sites on the surface of dicarboxymethyl cellulose.

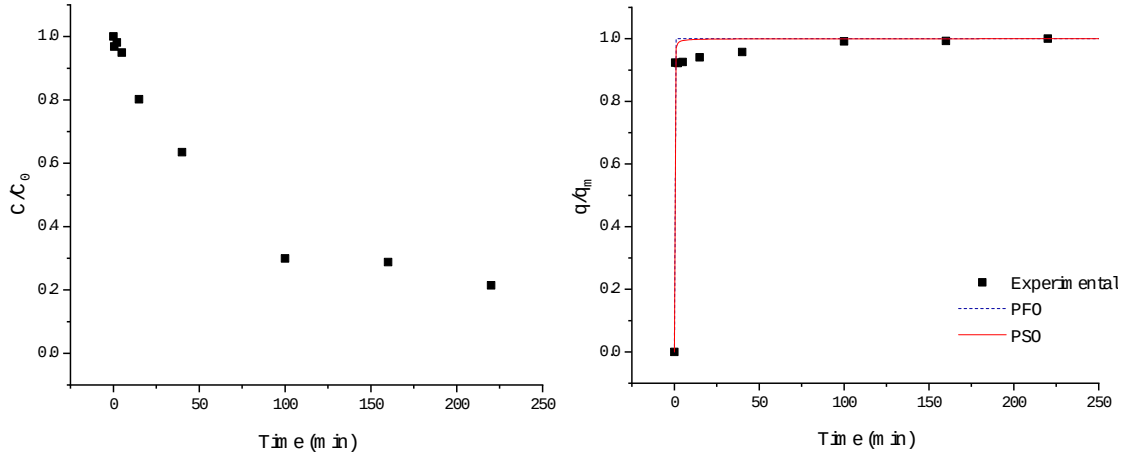

(a) (b)

Figure 4.4: Adsorption kinetics of a 20 mg/L Cytochrome *C* solution at pH = 7.2 onto DCMC 3 represented by normalized a) concentration and b) adsorption capacity.

Adsorption capacity of Cytochrome *C* onto dicarboxymethyl cellulose was calculated by $q = \frac{(C_0 - C_e)\,V}{m}$. The process was modeled with pseudo first-order and pseudo second-order kinetic models. The kinetic parameters for the adsorption of Cytochrome *C* onto DCMC 3 are displayed in Table 4.3. Both kinetic models present high correlation coefficients ($R^2 \geqslant 0.990$). However, since maximum adsorption capacity calculated by the pseudo second-order model is closer to experimental values (181.7 versus 188.0 mg/g, respectively), it is considered that this model adjusts better to experimental data.

4.4.5 Reusability study

The reusability experiments were performed with the polymer with better removal efficiencies. A 20 mg/L solution was added to 6 mg of DCMC 3. After three hours, the

Table 4.3: Adsorption kinetics parameters

		Pseudo first order			Pseudo second order		
Sample	pH	K_1 (min $^{-1}$)	q_m (mg/g)	R^2	K_2 (mg g^{-1} min^{-1})	q_m (mg/g)	R^2
DCMC 3	7.2	223.1±0.0	179.8±2.2	0.990	0.180±0.105	181.7±2.1	0.993

polymer was washed with deionized water and 1 M NaCl was added. The experiment was conducted over three cycles. The results on regeneration and reusability of dicarboxymethyl cellulose are shown in Figure 4.5.

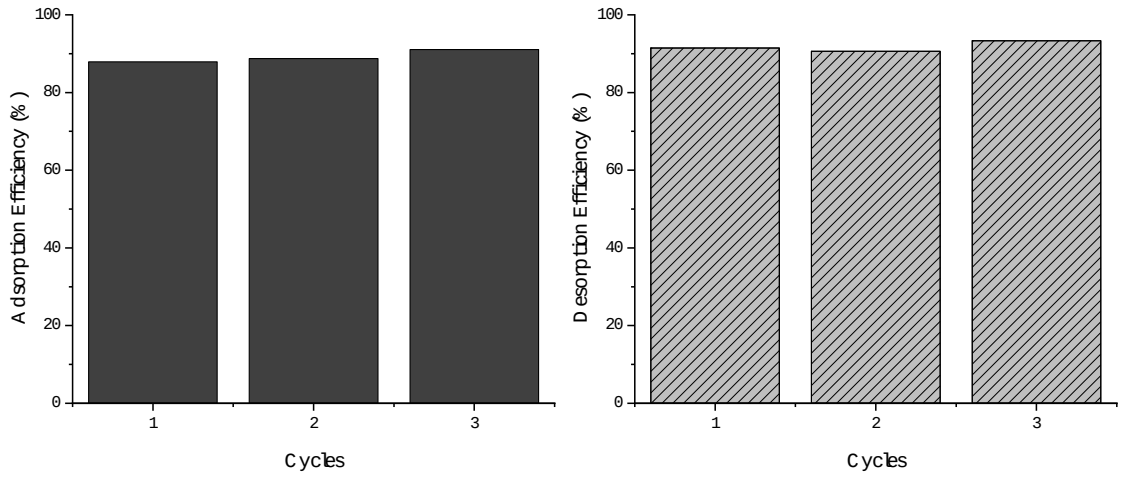

Figure 4.5: Removal efficiency for different adsorption-desorption cycles (adsorbent dosage: 1 mg/mL, pH = 7.2) represented by a) adsorption and b) desorption efficiency.

After three cycles, adsorption and desorption efficiencies remain unaffected. Adsorption efficiency ranged from 88 to 91%, while desorption exceeded 90% in all cycles. Since there is close to full desorption in each cycle, it is assumed that Cyt *C* is almost entirely removed. The lack of positively-charged proteins on the surface of the adsorbent reduce electrostatic repulsion between adsorbate and adsorbent, contributing to high adsorption efficiencies. Complete desorption of Cyt *C* may be explained by weak attraction between the protein and dicarboxymethyl cellulose. The use of NaCl as eluent agent proved to be successful.

4.4.6 Competitive adsorption of cytochrome *C* and lysozyme

Adsorptions experiments of cytochrome *C* and lysozyme were performed with two polymer dosages. Selective and competitive adsorption experiments were performed in phosphate buffer solution (pH = 7.2). 200 mg/L solutions of Cyt *C* and Lys were added to dicarboxymethyl cellulose. Similaly to previous experiments, the polymer with higher number of carboxylate groups (DCMC 3) was used. Lys was used as a reference protein

due to its similarities with Cyt C. The adsorption parameters for both proteins are presented in Tables 4.4 and 4.5.

In selective adsorption, Cyt *C* and Lys were added separately to the polymer. As expected, since Cyt *C* and Lys are similar in size and isoelectric point, selectivity was not observed. Polymer dosage did not affect the experiment, with removal efficiencies of 97 and 93% for Cyt *C* and Lys at a low dosage.

Table 4.4: Selective adsorption of Cyt *C* and Lys onto dicarboxymethyl cellulose

	Cyt *C*		Lys	
Dosage (mg/mL)	0.50	1	0.50	1
Removal Efficiency (%)	97.01	96.30	88.95	92.69

In the competitive adsorption experiments, dicarboxymethyl cellulose was in contact with both solutions at the same time. Results showed that both proteins had removal efficiencies over 85%. Once again, polymer dosage did not influence the results. Coadsorption of Cyt *C* and Lys did not reveal competition for binding sites.

Table 4.5: Competitive adsorption of Cyt *C* and Lys onto dicarboxymethyl cellulose

	Cyt *C*		Lys	
Dosage (mg/mL)	0.50	1	0.50	1
Removal Efficiency (%)	94.19	96.87	91.71	86.06

In both experiments, cation-exchange between the proteins and the adsorbent occurs. An experiment using a negatively-charged protein at the studied pH (lower isoelectric point) could demonstrate the charge-sensitive ion-exchange process. α-Lactalbumin (α-LA, MW = 14.2 kDa, pI = 4-5) has comparable size to Cyt *C* and Lys and an isoelectric point quite below the solution pH (Permyakov and Berliner, 2000). Therefore, α-LA would be completely deprotonated at pH = 7.2 and could be used for the proposed experiment.

4.5 Conclusions

Dicarboxymethyl cellulose was used for the adsorption of Cytochrome *C*. Results showed that increasing adsorbent dosage beyond 0.25 mg/mL did not affect removal efficiency. At this dosage, all samples removed above 90% of the protein. Adsorption efficiency increased with number of carboxylate groups per gram of polymer. Experimental data was adjusted to Langmuir isotherm model with a maximum protein uptake of 1279.6 mg/g. Kinetic studies showed that the experimental data was well described by pseudo second-order model. Cyt *C* is rapidly removed in the first 100 min. Selective and competitive adsorption studies did not display preferential equilibrium uptake of either

protein nor did it affect adsorption capacity. Reusability studies showed promising results. After three cycles, adsorption efficiency was above 90%. These results make dicarboxymethyl cellulose an ideal candidate for protein purification and separation.

The separation of positively-charged proteins, such as Cyt *C*, with this new cellulose-based polymer is promising. Future work should include the use of DCMC in Ion Exchange Chromatography. Also, selective and competitive studies using opposite charged proteins should be considered.

Chapter 5

Conclusions

In this work, the adsorption of dyes (Chapter 3) and proteins (Chapter 4) onto a new cellulose-based polymer was studied. The data obtained from these experiments allows for the evaluation of the potential of dicarboxymethyl cellulose as an adsorbent. The data gathered is of great importance since there is scarce information on the subject applied to this polymer.

Dicarboxymethyl cellulose was successfully synthesized following the method described by Chagas et al., 2019; Ferreira et al., 2019.

Excellent results on the removal of methylene blue showed that dicarboxymethyl cellulose may be used as a water remediation tool. Maximum adsorption capacities of methylene blue onto dicarboxymethyl cellulose, but especially DCMC 3, are higher than those reported in literature. High adsorption capacities, biodegradability and easy disposal are some of the factors that announce DCMC as an alternative to conventional adsorbents, namely commercial activated carbon. The coupling of adsorption and membrane filtration allowed for complete pigment removal.

Protein separation was studied by using Cytochrome *C* as a model protein. Equilibrium adsorption studies revealed that beyond a critical dose of 0.25 mg/mL there was 90% protein removal. Two thirds of the protein were adsorbed in the first 100 min. Reusability studies showed that, after three cycles, adsorption and desorption efficiencies were above 90%.

Results showed that, in general, adsorption capacity increases with the number of carboxylate groups per gram of polymer. The availability of binding sites contributes to the cation exchange between dicarboxymethyl cellulose and the respective adsorbate.

Dicarboxymethyl cellulose showed satisfactory performance in all experiments when compared to other adsorbents. Since information on this polymer is lacking, further

characterization by solid state nuclear magnetic resonance and scanning electron microscopy is advised. Standardization of the polymer size via mechanical processing and its influence on adsorption capacity should be considered. Future studies should include adsorption coupled with membrane filtration in cross-flow mode. In cross-flow the particles are swept by the flow of the bulk solution, leaving a thinner deposited polymer layer, reducing concentration polarization. The use of dicarboxymethyl cellulose in Ion Exchange Chromatography should be evaluated. It would also be interesting to study methylene blue adsorption at pH = 6.4 in a buffered solution and observe if there are changes in the isotherm shape.

Bibliography

Abramian, L. and H. El-Rassy (2009). "Adsorption kinetics and thermodynamics of azo-dye Orange II onto highly porous titania aerogel." In: *Chemical Engineering Journal* 150, pp. 403–410. ISSN: 13858947. DOI: 10.1016/j.cej.2009.01.019.

Aksu, Z. (2005). "Application of biosorption for the removal of organic pollutants: A review." In: *Process Biochemistry* 40, pp. 997–1026. ISSN: 00329592. DOI: 10.1016/j.procbio.2004.04.008.

Alberts, B., A. Johnson, J. Lewis, P. Walter, M. Raff, and K. Roberts (2002). *Molecular Biology of the Cell 4th Edition: International Student Edition*. Routledge. ISBN: 9780815332886. URL: https://books.google.pt/books?id=ozigkQEACAAJ.

Anastas, P. and N. Eghbali (2010). "Green chemistry: Principles and practice." In: *Chemical Society Reviews* 39 (1), pp. 301–312. ISSN: 03060012. DOI: 10.1039/b918763b.

Anirudhan, T. S. and S. S. Sreekumari (2010). "Synthesis and characterization of a functionalized graft copolymer of densified cellulose for the extraction of uranium(VI) from aqueous solutions." In: *Colloids and Surfaces A: Physicochemical and Engineering Aspects* 361, pp. 180–186. ISSN: 09277757. DOI: 10.1016/j.colsurfa.2010.03.031.

Anirudhan, T. S., A. R. Tharun, and S. R. Rejeena (2011). "Investigation on poly(metha crylic acid)-grafted cellulose/bentonite superabsorbent composite: Synthesis, Characterization, and adsorption characteristics of bovine serum albumin." In: *Industrial and Engineering Chemistry Research* 50 (4), pp. 1866–1874. ISSN: 08885885. DOI: 10.1021/ie101918m.

Aquino, L., E. Miranda, I. Duarte, P. Rosa, and S. Bueno (Sept. 2003). "Adsorption of human immunoglobulin G onto ethacrylate and histidine-linked methacrylate." en. In: *Brazilian Journal of Chemical Engineering* 20, pp. 251 –262. ISSN: 0104-6632. URL: http://www.scielo.br/scielo.php?script=sci_arttext&pid=S0104-66322003000300005&nrm=iso.

Bansal, R. C. and M. Goyal (2005). *Activated carbon adsorption*. CRC press.

Bellezza, F., A. Cipiciani, L. Latterini, T. Posati, and P. Sassi (2009). "Structure and catalytic behavior of myoglobin adsorbed onto nanosized hydrotalcites." In: *Langmuir* 25 (18), pp. 10918–10924. ISSN: 07437463. DOI: 10.1021/la901448a.

Bergaoui, M., A. Nakhli, Y. Benguerba, M. Khalfaoui, A. Erto, F. E. Soetaredjo, S. Ismadji, and B. Ernst (2018). "Novel insights into the adsorption mechanism of methylene blue

onto organo-bentonite: Adsorption isotherms modeling and molecular simulation." In: *Journal of Molecular Liquids* 272, pp. 697–707. ISSN: 01677322. DOI: 10.1016/j.molliq.2018.10.001.

Berizi, Z., S. Y. Hashemi, M. Hadi, A. Azari, and A. H. Mahvi (2016). "The study of non-linear kinetics and adsorption isotherm models for Acid Red 18 from aqueous solutions by magnetite nanoparticles and magnetite nanoparticles modified by sodium alginate." In: *Water Science and Technology* 74 (5), pp. 1235–1242. ISSN: 02731223. DOI: 10.2166/wst.2016.320.

Bhushan, B. (2013). *Introduction to Tribology*. Tribology in Practice Series. Wiley. ISBN: 9781118403228. URL: https://books.google.pt/books?id=DJDv5jVwC2UC.

Bonner, P. (2007). *Protein Purification*. The Basics (Garland Science). Taylor & Francis. ISBN: 9780203967263. URL: https://books.google.pt/books?id=0nN_fn4e9PgC.

Bulut, Y. and H. Aydin (2006). "A kinetics and thermodynamics study of methylene blue adsorption on wheat shells." In: *Desalination* 194, pp. 259–267. ISSN: 00119164. DOI: 10.1016/j.desal.2005.10.032.

Cao, J., J. Zhang, Y. Zhu, S. Wang, X. Wang, and K. Lv (2018). "Novel Polymer Material for Efficiently Removing Methylene Blue, Cu(II) and Emulsified Oil Droplets from Water Simultaneously." In: *Polymers* 10 (12), p. 1393. DOI: 10.3390/polym10121393.

Cecen, F. and Ö. Aktas (2011). *Activated Carbon for Water and Wastewater Treatment: Integration of Adsorption and Biological Treatment*. Wiley. ISBN: 9783527639458. URL: https://books.google.pt/books?id=ubVxmXZ0j8wC.

Chagas, R., M. Gericke, R. B. Ferreira, T. Heinze, and L. M. Ferreira (2019). "Synthesis and characterization of dicarboxymethyl cellulose." Manuscript submitted for publication.

Choi, J. G., D. D. Do, and H. D. Do (2001). "Surface diffusion of adsorbed molecules in porous media: Monolayer, multilayer, and capillary condensation regimes." In: *Industrial and Engineering Chemistry Research* 40 (19), pp. 4005–4031. ISSN: 08885885. DOI: 10.1021/ie010195z.

Cobzaru, C. and V. Inglezakis (2015). *Progress in Filtration and Separation: Chapter Ten - Ion Exchange*. Elsevier Ltd, pp. 425–498. ISBN: 9780123847461. DOI: 10.1016/B978-0-12-384746-1.00010-0.

Colangelo, D., F. Torchio, D. M. De Faveri, and M. Lambri (2018). "The use of chitosan as alternative to bentonite for wine fining: Effects on heat-stability, proteins, organic acids, colour, and volatile compounds in an aromatic white wine." In: *Food Chemistry* 264, pp. 301–309. ISSN: 18737072. DOI: 10.1016/j.foodchem.2018.05.005.

Devasahayam, S., S. Bandyopadhyay, and D. J. Hill (2016). "Study of Victorian Brown Coal Dewatering by Super Absorbent Polymers using Attenuated Total Reflection Fourier Transform Infrared Spectroscopy." In: *Mineral Processing and Extractive Metallurgy Review* 37 (4), pp. 220–226. ISSN: 15477401. DOI: 10.1080/08827508.2016.1168417.

Diamantoglou, M, H Mägerlein, and R Zielke (1977). "Polycarboxylate aus Polysacchariden, Holz und holzähnlich zusammengesetzten Stoffen als neuartige Sequestriermittel." In: *Tenside Detergents* 14, pp. 250–256.

Dąbrowski, A. (2001). "Adsorption - from theory to practice." In: *Advances in Colloid and Interface Science* 93, pp. 135–224. ISSN: 00018686. DOI: 10.1016/S0001-8686(00)00082-8.

Everett, D. (1972). "Manual of symbols and terminology for physicochemical quantities and units." In: *International Union of Pure and Applied Chemistry* 31, pp. 579–638. DOI: 10.1351/pac197231040577.

Febrianto, J., A. N. Kosasih, J. Sunarso, Y. H. Ju, N. Indraswati, and S. Ismadji (2009). "Equilibrium and kinetic studies in adsorption of heavy metals using biosorbent: A summary of recent studies." In: *Journal of Hazardous Materials* 162, pp. 616–645. ISSN: 03043894. DOI: 10.1016/j.jhazmat.2008.06.042.

Feng, Z., Z. Shao, J. Yao, Y. Huang, and X. Chen (2009). "Protein adsorption and separation with chitosan-based amphoteric membranes." In: *Polymer* 50 (5), pp. 1257–1263. ISSN: 00323861. DOI: 10.1016/j.polymer.2008.12.046.

Ferreira, L. M., R. Chagas, R. B. Ferreira, I. Coelhoso, and S. Velizarov (2019). *Compound, method of production and uses thereof*. Patent Application PCT/IB2018/052632.

Friedrich, F. and P. G. Weidler (2010). "Contact pressure effects on vibrational bands of kaolinite during infrared spectroscopic measurements in a diamond attenuated total reflection cell." In: *Applied Spectroscopy* 64 (5), pp. 500–506. ISSN: 00037028. DOI: 10.1366/000370210791211619.

Furia, T. (1973). *CRC Handbook of Food Additives, Second Edition*. Vol. 1. Taylor & Francis, pp. 320–324. ISBN: 9780849305429. URL: https://books.google.pt/books?id=XcSp015g4X0C.

Gregg, S. and K. Sing (1991). *Adsorption, surface area, and porosity*. Academic Press. ISBN: 9780123009562. URL: https://books.google.pt/books?id=YhNRAAAAMAAJ.

Guthrie, J. D. and A. L. Bullock (1960). "Ion Exchange Celluloses for Chromatographic Separations." In: *Industrial and Engineering Chemistry* 52 (11), pp. 935–937. ISSN: 00197866. DOI: 10.1021/ie50611a028.

Hamdaoui, O. and E. Naffrechoux (2007). "Modeling of adsorption isotherms of phenol and chlorophenols onto granular activated carbon. Part II. Models with more than two parameters." In: *Journal of Hazardous Materials* 147, pp. 401–411. ISSN: 03043894. DOI: 10.1016/j.jhazmat.2007.01.023.

Harrison, R., P. Todd, S. Rudge, and D. Petrides (2015). *Bioseparations Science and Engineering*. Topics in chemical engineering. Oxford University Press. ISBN: 9780195391817. URL: https://books.google.pt/books?id=15IKBgAAQBAJ.

Heinze, T., O. Seoud, and A. Koschella (2018). *Cellulose Derivatives: Synthesis, Structure, and Properties*. Springer Series on Polymer and Composite Materials. Springer International Publishing. ISBN: 9783319731681. URL: https://books.google.pt/books?id=0uBLDwAAQBAJ.

Ho, Y.-S. (2004). "Citation review of Lagergren kinetic rate equation on adsorption reactions." In: *Scientometrics* 59 (1), pp. 171–177. ISSN: 01389130. DOI: 10.1023/B:SCIE.0000013305.99473.cf.

Huang, L.-C. L. and H.-C. Chang (2004). "Adsorption and Immobilization of Cytochrome c on Nanodiamonds." In: *Langmuir* 20 (14), pp. 5879–5884. DOI: 10.1021/la0495736.

Inglezakis, V. J., S. G. Poulopoulos, and H. Kazemian (2018). "Insights into the S-shaped sorption isotherms and their dimensionless forms." In: *Microporous and Mesoporous Materials* 272, pp. 166–176. ISSN: 13871811. DOI: 10.1016/j.micromeso.2018.06.026.

Kahr, G. and F. T. Madsen (1995). "Determination of the cation exchange capacity and the surface area of bentonite, illite and kaolinite by methylene blue adsorption." In: *Applied Clay Science* 9 (5), pp. 327–336. ISSN: 01691317. DOI: 10.1016/0169-1317(94)00028-0.

Kannan, N. and M. M. Sundaram (2001). "Kinetics and mechanism of removal of methylene blue by adsorption on various carbons—a comparative study." In: *Dyes and Pigments* 51 (1), pp. 25–40. ISSN: 0143-7208. DOI: 10.1016/S0143-7208(01)00056-0.

Khodaie, M., N. Ghasemi, B. Moradi, and M. Rahimi (2013). "Removal of methylene blue from wastewater by adsorption onto znclactivated corn husk carbon equilibrium studies." In: *Journal of Chemistry* 2013. ISSN: 20909063. DOI: 10.1155/2013/383985.

Kirk-Othmer (2005). *Kirk-Othmer Encyclopedia of Chemical Technology*. Wiley.

Klemm, D., B. Heublein, H. P. Fink, and A. Bohn (2005). "Cellulose: Fascinating biopolymer and sustainable raw material." In: *Angewandte Chemie - International Edition* 44 (22), pp. 3358–3393. ISSN: 14337851. DOI: 10.1002/anie.200460587.

Kondo, A. and K. Higashitani (1992). "Adsorption of model proteins with wide variation in molecular properties on colloidal particles." In: *Journal of Colloid And Interface Science* 150 (2), pp. 344–351. ISSN: 00219797. DOI: 10.1016/0021-9797(92)90204-Y.

Kötz, J, I Nehls, B Philipp, and M Diamantoglou (1991). "Zum Polyelektrolytverhalten von Dicarboxymethylcellulose." In: *Das Papier* 45, pp. 226–231.

Kyzas, G. Z. and M. Kostoglou (2014). "Green adsorbents for wastewaters: A critical review." In: *Materials* 7 (1), pp. 333–364. ISSN: 19961944. DOI: 10.3390/ma7010333.

Largitte, L. and R. Pasquier (2016). "A review of the kinetics adsorption models and their application to the adsorption of lead by an activated carbon." In: *Chemical Engineering Research and Design* 109, pp. 495–504. ISSN: 02638762. DOI: 10.1016/j.cherd.2016.02.006.

Li, L., X. Sun, and B. Li (2012). "Adsorption of cytochrome c by succinic anhydride-modified peanut shells." In: *Advances in Bioscience and Biotechnology* 03 (1), pp. 14–19. ISSN: 2156-8456. DOI: 10.4236/abb.2012.31003.

Li, Z., P. Guan, X. Hu, S. Ding, Y. Tian, Y. Xu, and L. Qian (2018). "Preparation of molecularly imprinted mesoporous materials for highly enhancing adsorption performance of Cytochrome C." In: *Polymers* 10 (3). ISSN: 20734360. DOI: 10.3390/polym10030298.

Lima, É. C., M. A. Adebayo, and F. M. Machado (2015). "Kinetic and Equilibrium Models of Adsorption." In: *Carbon Nanomaterials as Adsorbents for Environmental and Biological Applications*. Ed. by C. P. Bergmann and F. M. Machado. Cham: Springer International Publishing, pp. 33–69. ISBN: 978-3-319-18875-1. DOI: 10.1007/978-3-319-18875-1_3.

Lin, Q., M. Gao, J. Chang, and H. Ma (2017). "Highly effective adsorption performance of carboxymethyl cellulose microspheres crosslinked with epichlorohydrin." In: *Journal of Applied Polymer Science* 134 (2). ISSN: 10974628. DOI: 10.1002/app.44363.

Liu, C., A. M. Omer, and X. kun Oug (2018). "Adsorptive removal of cationic methylene blue dye using carboxymethyl cellulose/k-carrageenan/activated montmorillonite composite beads: Isotherm and kinetic studies." In: *International Journal of Biological Macromolecules* 106, pp. 823–833. ISSN: 18790003. DOI: 10.1016/j.ijbiomac.2017.08.084.

Missoum, K., M. N. Belgacem, and J. Bras (2013). "Nanofibrillated cellulose surface modification: A review." In: *Materials* 6 (5), pp. 1745–1766. ISSN: 19961944. DOI: 10.3390/ma6051745.

Mitrogiannis, D., G. Markou, A. Çelekli, and H. Bozkurt (2015). "Biosorption of methylene blue onto Arthrospira platensis biomass: Kinetic, equilibrium and thermodynamic studies." In: *Journal of Environmental Chemical Engineering* 3 (2), pp. 670–680. ISSN: 22133437. DOI: 10.1016/j.jece.2015.02.008.

Miyahara, M., A. Vinu, and K. Ariga (2007). "Adsorption myoglobin over mesoporous silica molecular sieves: Pore size effect and pore-filling model." In: *Materials Science and Engineering C* 27 (2), pp. 232–236. ISSN: 09284931. DOI: 10.1016/j.msec.2006.05.012.

Moore, G. (2012). *Introduction to Inductively Coupled Plasma Atomic Emission Spectrometry*. Analytical Spectroscopy Library. Elsevier Science. ISBN: 9780444599070. URL: https://books.google.pt/books?id=Q5ZCLru_ckEC.

Mouni, L., L. Belkhiri, J. C. Bollinger, A. Bouzaza, A. Assadi, A. Tirri, F. Dahmoune, K. Madani, and H. Remini (2018). "Removal of Methylene Blue from aqueous solutions by adsorption on Kaolin: Kinetic and equilibrium studies." In: *Applied Clay Science* 153, pp. 38–45. ISSN: 01691317. DOI: 10.1016/j.clay.2017.11.034.

Nasatto, P. L., F. Pignon, J. L. Silveira, M. E. R. Duarte, M. D. Noseda, and M. Rinaudo (2015). "Methylcellulose, a cellulose derivative with original physical properties and extended applications." In: *Polymers* 7 (5), pp. 777–803. ISSN: 20734360. DOI: 10.3390/polym7050777.

Novais, R. M., G. Ascensão, D. M. Tobaldi, M. P. Seabra, and J. A. Labrincha (2018a). "Biomass fly ash geopolymer monoliths for effective methylene blue removal from

wastewaters." In: *Journal of Cleaner Production* 171, pp. 783–794. ISSN: 09596526. DOI: 10.1016/j.jclepro.2017.10.078.

Novais, R. M., A. P. F. Caetano, M. P. Seabra, J. A. Labrincha, and R. C. Pullar (2018b). "Extremely fast and efficient methylene blue adsorption using eco-friendly cork and paper waste-based activated carbon adsorbents." In: *Journal of Cleaner Production* 197, pp. 1137–1147. ISSN: 0959-6526. DOI: 10.1016/j.jclepro.2018.06.278.

Onwukamike, K. N., S. Grelier, E. Grau, H. Cramail, and M. A. Meier (2019). "Critical Review on Sustainable Homogeneous Cellulose Modification: Why Renewability Is Not Enough." In: *ACS Sustainable Chemistry and Engineering* 7 (2), pp. 1826–1840. ISSN: 21680485. DOI: 10.1021/acssuschemeng.8b04990.

Perkin-Elmer. *Perkin-Elmer Manual*. The Effects of Varying Force and Contact on ATR Spectra. Perkin-Elmer.

Permyakov, E. A. and L. J. Berliner (2000). "α-Lactalbumin: structure and function." In: *FEBS Letters* 473 (3), pp. 269–274. ISSN: 00145793. DOI: 10.1016/S0014-5793(00)01546-5.

Peterson, E. A. and H. A. Sober (1956). "Chromatography of Proteins. I. Cellulose Ion-Exchange Adsorbents." In: *Journal of the American Chemical Society* 78 (4), pp. 751–755. ISSN: 15205126. DOI: 10.1021/ja01585a016.

Qiao, L., L. Zhao, H. Ai, Y. Li, Y. Liu, and K. Du (2019). "Diethylaminoethyl-Modified Magnetic Starlike Organic Spherical Adsorbent: Fabrication, Characterization, and Potential for Protein Adsorption." In: *Industrial and Engineering Chemistry Research* 58 (10), pp. 4099–4107. ISSN: 15205045. DOI: 10.1021/acs.iecr.8b05967.

Rafatullah, M., O. Sulaiman, R. Hashim, and A. Ahmad (2010). "Adsorption of methylene blue on low-cost adsorbents: A review." In: *Journal of Hazardous Materials* 177, pp. 70–80. ISSN: 03043894. DOI: 10.1016/j.jhazmat.2009.12.047.

Rehman, I. and W. Bonfield (1997). "Characterization of hydroxyapatite and carbonated apatite by photo acoustic FTIR spectroscopy." In: *Journal of Materials Science: Materials in Medicine* 8 (1), pp. 1–4. ISSN: 09574530. DOI: 10.1023/A:1018570213546.

Ren, B., Y. Xu, L. Zhang, and Z. Liu (2018). "Carbon-doped graphitic carbon nitride as environment-benign adsorbent for methylene blue adsorption: Kinetics, isotherm and thermodynamics study." In: *Journal of the Taiwan Institute of Chemical Engineers* 88, pp. 114–120. ISSN: 18761070. DOI: 10.1016/j.jtice.2018.03.041.

Ren, H., Z. Gao, D. Wu, J. Jiang, Y. Sun, and C. Luo (2016). "Efficient Pb(II) removal using sodium alginate-carboxymethyl cellulose gel beads: Preparation, characterization, and adsorption mechanism." In: *Carbohydrate Polymers* 137 (2), pp. 402–409. ISSN: 01448617. DOI: 10.1016/j.carbpol.2015.11.002.

Rouquerol, J., F. Rouquerol, P. Llewellyn, G. Maurin, and K. Sing (2013). *Adsorption by Powders and Porous Solids: Principles, Methodology and Applications*. Elsevier Science. ISBN: 9780080970363. URL: https://books.google.pt/books?id=U0E-ZscCYncC.

Roy, D., M. Semsarilar, J. T. Guthrie, and S. Perrier (2009). "Cellulose modification by polymer grafting: A review." In: *Chemical Society Reviews* 38 (7), pp. 2046–2064. ISSN: 03060012. DOI: 10.1039/b808639g.

Saber-Samandari, S., S. Saber-Samandari, S. Heydaripour, and M. Abdouss (2016). "Novel carboxymethyl cellulose based nanocomposite membrane: Synthesis, characterization and application in water treatment." In: *Journal of Environmental Management* 166, pp. 457–465. ISSN: 10958630. DOI: 10.1016/j.jenvman.2015.10.045.

Senthil Kumar, P., S. Ramalingam, C. Senthamarai, M. Niranjanaa, P. Vijayalakshmi, and S. Sivanesan (2010). "Adsorption of dye from aqueous solution by cashew nut shell: Studies on equilibrium isotherm, kinetics and thermodynamics of interactions." In: *Desalination* 261, pp. 52–60. ISSN: 00119164. DOI: 10.1016/j.desal.2010.05.032.

Sigma-Aldrich. *Sigma-Aldrich Product Information*. Cytochrome C from equine heart. Sigma-Aldrich.

Singha, B. and S. K. Das (2013). "Adsorptive removal of Cu(II) from aqueous solution and industrial effluent using natural/agricultural wastes." In: *Colloids and Surfaces B: Biointerfaces* 107, pp. 97–106. ISSN: 09277765. DOI: 10.1016/j.colsurfb.2013.01.060.

Smith, B. (2011). *Fundamentals of Fourier Transform Infrared Spectroscopy*. CRC Press. ISBN: 9781420069303. URL: https://books.google.pt/books?id=LR9HkK2cP_0C.

Ståhlberg, J. (1994). "Electrostatic Retention Model for Ion-Exchange Chromatography." In: *Analytical Chemistry* 66 (4), pp. 440–449. ISSN: 15206882. DOI: 10.1021/ac00076a005.

Suhas, V. K. Gupta, P. J. Carrott, R. Singh, M. Chaudhary, and S. Kushwaha (2016). "Cellulose: A review as natural, modified and activated carbon adsorbent." In: *Bioresource Technology* 216, pp. 1066–1076. ISSN: 18732976. DOI: 10.1016/j.biortech.2016.05.106.

Sun, P., S. Yang, X. Sun, Y. Wang, L. Pan, H. Wang, X. Wang, J. Guo, and C. Nie (2019). "Functional Porous Carboxymethyl Cellulose/Cellulose Acetate Composite Microspheres: Preparation, Characterization, and Application in the Effective Removal of HCN from Cigarette Smoke." In: *Polymers* 11 (1), p. 181. DOI: 10.3390/polym11010181.

Takeda, K., T. Uchihashi, H. Watanabe, T. Ishida, K. Igarashi, N. Nakamura, and H. Ohno (2015). "Real-time dynamic adsorption processes of cytochrome c on an electrode observed through electrochemical high-speed atomic force microscopy." In: *PLoS ONE* 10 (2), pp. 1–10. ISSN: 19326203. DOI: 10.1371/journal.pone.0116685.

Thompson, M. (2012). *Handbook of Inductively Coupled Plasma Spectrometry: Second Edition*. Springer US. ISBN: 9781461306979. URL: https://books.google.pt/books?id=8psyBwAAQBAJ.

Tien, C. (2018). *Introduction to Adsorption: Basics, Analysis, and Applications*. Elsevier Science. ISBN: 9780128175125. URL: https://books.google.pt/books?id=Anx8DwAAQBAJ.

Tsai, J. H., H. M. Chiang, G. Y. Huang, and H. L. Chiang (2008). "Adsorption characteristics of acetone, chloroform and acetonitrile on sludge-derived adsorbent, commercial granular activated carbon and activated carbon fibers." In: *Journal of Hazardous Materials* 154, pp. 1183–1191. ISSN: 03043894. DOI: 10.1016/j.jhazmat.2007.11.065.

Van Sluyter, S. C., J. M. McRae, R. J. Falconer, P. A. Smith, A. Bacic, E. J. Waters, and M. Marangon (2015). "Wine protein haze: Mechanisms of formation and advances in prevention." In: *Journal of Agricultural and Food Chemistry* 63 (16). ISSN: 15205118. DOI: 10.1021/acs.jafc.5b00047.

Varshney, V. K. and S. Naithani (2011). "Cellulose Fibers: Bio- and Nano-Polymer Composites." In: *Cellulose Fibers: Bio- and Nano-Polymer Composites* 63, pp. 43–60. DOI: 10.1007/978-3-642-17370-7.

Varshney, V. K., P. K. Gupta, S. Naithani, R. Khullar, A. Bhatt, and P. L. Soni (2006). "Carboxymethylation of α-cellulose isolated from Lantana camara with respect to degree of substitution and rheological behavior." In: *Carbohydrate Polymers* 63 (1), pp. 40–45. ISSN: 01448617. DOI: 10.1016/j.carbpol.2005.07.001.

Vela, E., P. Hernández-Orte, E. Castro, V. Ferreira, and R. Lopez (2017). "Effect of bentonite fining on polyfunctional mercaptans and other volatile compounds in Sauvignon blanc wines." In: *American Journal of Enology and Viticulture* 68 (1), pp. 30–38. ISSN: 00029254. DOI: 10.5344/ajev.2016.16052.

Vilela, C., C. S. Freire, P. A. Marques, T. Trindade, C. Pascoal Neto, and P. Fardim (2010). "Synthesis and characterization of new CaCO3/cellulose nanocomposites prepared by controlled hydrolysis of dimethylcarbonate." In: *Carbohydrate Polymers* 79 (4), pp. 1150–1156. ISSN: 01448617. DOI: 10.1016/j.carbpol.2009.10.056.

Vinu, A, V Murugesan, O. Tangermann, and M. Hartmann (2004). "Adsorption of Cytochrome c on Mesoporous Molecular Sieves: Influence of pH, Pore Diameter, and Aluminum Incorporation." In: *Chemistry of Materials* 16, pp. 3056–3065. DOI: 10.1021/cm049718u.

Volesky, B. (2003). "Biosorption process simulation tools." In: *Hydrometallurgy* 71, pp. 179–190. ISSN: 0304386X. DOI: 10.1016/S0304-386X(03)00155-5.

Wankat, P. (2012). *Separation Process Engineering: Includes Mass Transfer Analysis*. Prentice Hall. ISBN: 9780131382275. URL: https://books.google.pt/books?id=p883u2-0w6cC.

Wankat, P. C. (1990). *Rate-controlled separations*. Elsevier Applied Science. ISBN: 9781851665211. URL: https://books.google.pt/books?id=J9ZTAAAAMAAJ.

Wuestenberg, T. (2014). *Cellulose and Cellulose Derivatives in the Food Industry: Fundamentals and Applications*. Wiley. ISBN: 9783527337583. URL: https://books.google.pt/books?id=pAUeCgAAQBAJ.

Xiao, P., J. Zhang, Y., J. Wu, J. He, and J. Zhang (2014). "Synthesis, characterization and properties of novel cellulose derivatives containing phosphorus: Cellulose diphenyl phosphate and its mixed esters." In: *Cellulose* 21 (4), pp. 2369–2378. ISSN: 09690239. DOI: 10.1007/s10570-014-0256-9.

Xin, P. P., Y. B. Huang, C. Y. Hse, H. N. Cheng, C. Huang, and H. Pan (2017). "Modification of cellulose with succinic anhydride in TBAA/DMSO mixed solvent under catalyst-free conditions." In: *Materials* 10 (5). ISSN: 19961944. DOI: 10.3390/ma10050526.

Yan, H., W. Zhang, X. Kan, L. Dong, Z. Jiang, H. Li, H. Yang, and R. Cheng (2011). "Sorption of methylene blue by carboxymethyl cellulose and reuse process in a secondary sorption." In: *Colloids and Surfaces A: Physicochemical and Engineering Aspects* 380, pp. 143–151. ISSN: 09277757. DOI: 10.1016/j.colsurfa.2011.02.045.

Zeng, X. and E. Ruckenstein (1998). "Cross-linked macroporous chitosan anion-exchange membranes for protein separations." In: *Journal of Membrane Science* 148 (2), pp. 195–205. ISSN: 03767388. DOI: 10.1016/S0376-7388(98)00183-5.

Zhao, S. and T. Zhou (2016). "Biosorption of methylene blue from wastewater by an extraction residue of Salvia miltiorrhiza Bge." In: *Bioresource Technology* 219, pp. 330–337. ISSN: 18732976. DOI: 10.1016/j.biortech.2016.07.121.